

Accepted Manuscript

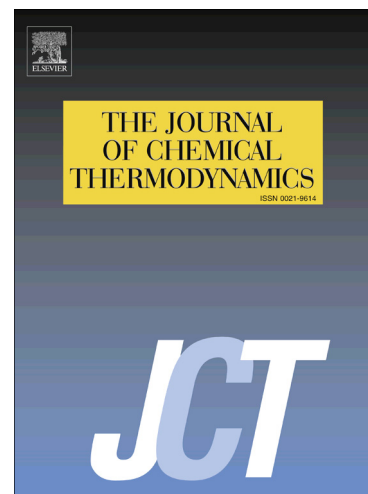
Investigation of solute-solvent interactions in {1-butyl-3-methyl imidazolium-Bis(trifluoromethylsulfonyl)imide+dimethylcarbonate} mixture using physico-chemical properties

V. Srinivasa Rao, M. Srinivasa Reddy, Sk. MdNayeem, K. Thomas S.S. Raju, K. Bala Murali Krishna, B. Hari Babu

PII: S0021-9614(17)30238-0
DOI: <http://dx.doi.org/10.1016/j.jct.2017.07.013>
Reference: YJCHT 5131

To appear in: *J. Chem. Thermodynamics*

Received Date: 25 April 2017
Revised Date: 20 June 2017
Accepted Date: 6 July 2017



Please cite this article as: V. Srinivasa Rao, M. Srinivasa Reddy, Sk. MdNayeem, K.T.S.S. Raju, K. Bala Murali Krishna, B. Hari Babu, Investigation of solute-solvent interactions in {1-butyl-3-methyl imidazoliumBis(trifluoromethylsulfonyl)imide+dimethylcarbonate} mixture using physicochemical properties, *J. Chem. Thermodynamics* (2017), doi: <http://dx.doi.org/10.1016/j.jct.2017.07.013>

This is a PDF file of an unedited manuscript that has been accepted for publication. As a service to our customers we are providing this early version of the manuscript. The manuscript will undergo copyediting, typesetting, and review of the resulting proof before it is published in its final form. Please note that during the production process errors may be discovered which could affect the content, and all legal disclaimers that apply to the journal pertain.

Investigation of solute-solvent interactions in {1-butyl-3-methylimidazoliumBis(trifluoromethylsulfonyl)imide+dimethylcarbonate} mixture using physicochemical properties

V. SrinivasaRao^{a,d}, M. SrinivasaReddy^b, Sk.MdNayeem^c, K.Thomas S S Raju^d, K. BalaMuraliKrishna^e, B. HariBabu^{*e}

^aDepartment of Chemistry, SRR & CVR Govt. Degree College, Vijayawada-520008, A.P., India.

^bDepartment of Chemistry, KRK Govt. Degree College, Addanki-523201, A.P., India.

^cDepartment of Physics, KRK Govt. Degree College, Addanki-523201, A.P., India.

^dDepartment of Chemistry, Andhra Loyola College, Vijayawada-520008, A.P., India.

^eDepartment of Chemistry, AcharyaNagarjuna University, Nagarjunanagar-522510, A.P., India.

ABSTRACT:

Physical properties, such as density (ρ), speed of sound (u) and refractive index of [Bmim][NTf₂], DMC and their binary mixtures are measured over the whole composition range as a function of temperature between (303.15 - 323.15) K at atmospheric pressure. Experimental values are used to calculate excess values of molar volumes (V_m^E)/partial molar volumes (\bar{V}_m^E)/partial molar volumes at infinite dilution ($\bar{V}_m^{E,\infty}$)/isentropic compressibility (κ_s^E)/free length (L_f^E), speed of sound (u^E) and isobaric thermal expansion coefficient (α_p^E) for the binary mixture. These excess properties are fitted to the Redlich-Kister equation to obtain the binary coefficients and the standard deviations. A qualitative analysis of these parameters indicates strong intermolecular interactions and the interaction increases with the increase in temperature. Further, through physicochemical properties, an attempt for calorimetric excess chemical potential using different equations is computed at $T=308.15\text{K}$. The present investigation also comprises of evaluation of the acoustic non-linearity parameter (B/A) in the mixtures and calculation of cohesive energy (ΔA), Van der Wall's constants (a , b), distance of closest approach (d). The presence of strong interactions is further supported by IR spectroscopy and the Prigogine-Flory-Patterson (PFP) theory.

Key words: [Bmim][NTf₂]; DMC; density; speed of sound; refractive index; excess thermodynamic parameters.

* Corresponding Author: dr.b.haribabu@gmail.com

Phone: +91-8500338866

1. Introduction

Substances that are entirely composed of ions with melting temperatures around 373 K are a family of Ionic liquids (ILs). Present days they attracted considerable attention because of their distinctive properties such as thermal stability, non-volatility and reusability [1,2]. Ionic liquids can be selected to have different anions and cations, so that one can form ionic liquid with the desired properties. ILs with special functional groups has been designed for application in many industrial processes. ILs are utilized for different purposes like extraction, separation and alternative solvents in catalytic reactions, synthesis, catalysis, biocatalyst, electro chemical devices, separation technology, reaction media, green solvents and in bio degradable materials.

Mixtures of ILs and molecular organic solvents are gaining interest of researchers as resultant liquid mixtures containing the advantages over both IL and molecular organic solvents. The properties of these mixtures are based on the mixing ratio. Mixing of the ILs with molecular solvents is one of the alternative steps to minimize the usage of expensive ILs and to save time for preparing new ILs [3]. From an economic and ecological perspective, the mixtures of ILs and traditional organic solvents may be gaining a tremendous amount of attention from both the researchers and the industries. Ionic liquids are more viscous than conventional organic solvents, which may hamper their application. Fortunately, their mixtures with molecular solvents show reduced viscosity without affecting their advantages as green solvents. In particular, the addition of polar co-solvents can strongly influence the physical and chemical properties of ILs such as viscosity, reactivity and electrical conductivity as well as solubility and solvation properties [4]. Recently, several binary IL+ molecular solvent systems have been shown to perform better than the pure ILs, and such systems have been used in numerous applications such as biocatalyzed reactions, as super capacitors, as reaction media, medium for dissolution of biopolymers etc. [5-17]. Hence, IL + molecular solvent mixtures have received growing attention in the past few years. The potential of these new substances can be exploited with experimental methods that can reliably predict the thermodynamic properties. Most of these novel media are characterized by their volumetric, acoustic and refractive index properties, since this data is important for industrial applications. To predict molecular interactions between binary liquids, speed of sound and refractive index along with experimental data of density plays vital role.

The choice of the investigated Ionic liquid, 1-butyl-3-methylimidazoliumbis (trifluoromethylsulfonyl)imide ([Bmim][NTf₂]) was on the basis of its ability to act as extracting solvent for the removal of many organic compounds through liquid-liquid extraction [18,19]. It is also widely used in catalysis [20] and chromatography [21]. On the other hand, dimethyl carbonate (DMC) can be a replacement of conventional organic solvents that damage the atmosphere. Moreover, DMC has been favoured as a green replacement for halogenated solvents due to its similarity with these types of liquids as well as ethers and esters [22]. Thus, one of the main properties of DMC is its ability to dissolve salts and particularly lithium ions. It contains high concentration of LiPF₆ and also used for high power density double-layer capacitors [23,24] and thus it represents a viable alternative to acetate esters and ketones in most applications, from paints to adhesives, taking advantage of its good solvency power [25]. Further, it is the file leader of many derived carbonic esters, available by transesterification reactions, whose properties can be tailored according to the target applications, like in the field of lubricating oils [26]. It is a non-aqueous electrolyte component and is finding increasing applications in the field of lithium rechargeable batteries, as witnessed by the number of patents in the area [27]. Additionally, it is used as a blowing agent in polyurethane foam after CFC ban [28].

Systematic investigation of the physicochemical properties of [Bmim][NTf₂] with molecular organic solvents including water have been reported. Alfonsina *et al* [29] reported the physicochemical properties such as density, refractive index, viscosity of [Bmim][NTf₂] binary mixture with ethanol or ethyl acetate. Zarrougui *et al* [30] reported the density, viscosity and conductivity and thermal expansivities of propylene carbonate with [Bmim][NTf₂], where as Widowati *et al* [31] reported pressure-volume-temperature properties of binary mixtures of the [Bmim][NTf₂] with anisole or acetophenone at elevated pressures. Vranes *et al* [32] reported density and excess properties of [Bmim][NTf₂]+Propylene carbonate binary mixtures, Monika *et al* [33] reported acoustic and volumetric properties of binary mixtures of [Bmim][NTf₂] with acetonitrile or tetrahydrofuran, Vranes *et al* [34] reported density, electrical conductivity and viscosity of binary liquid mixtures of [Bmim][NTf₂] with γ -butyrolactone (GBL), Salinas *et al* [35] reported densities, speed of sound, viscosity and excess properties of binary mixtures formed by ethanol and [Bmim][NTf₂], Jacquemin *et al* [36] reported the density and viscosity of several pure and water-saturated ionic liquids including [Bmim][NTf₂], Kassim *et al* [37]

reported the experimental densities and viscosities of binary mixture of [Bmim][NTf₂] with glycerol or sulfolane and their molecular interaction by COSMO-RS, Krishna *et al* [38] reported densities, speeds of sound and refractive indexes of the binary mixture of [Bmim][NTf₂] with pyrrolidin-2-one. But the thermo acoustic, volumetric and refractive index data of [Bmim][NTf₂] with DMC was not reported.

On the basis of our initial experiments, [Bmim][NTf₂] is found to be totally miscible with DMC in all proportions. Hence, in the present study, it is proposed to measure the densities, speeds of sound and refractive indexes of the binary mixtures of [Bmim][NTf₂] with DMC in the temperature range between (303.15-323.15) K in the entire composition range and at atmospheric pressure. On the basis of the measured values, we calculated the excess/deviation properties for their potential application in industrial processes. Here we reported the excess properties such as molar volumes (V_m^E), isentropic compressibilities (κ_s^E), free length (L_f^E), speeds of sound (u^E) and isobaric thermal expansion coefficient (α_p^E) along with $\left(\frac{\partial V_m^E}{\partial T}\right)_p$ and $\left(\frac{\partial H_m^E}{\partial P}\right)_T$. Besides, the deviation of refractive index on volume fraction basis ($\Delta_\phi n_D$) reported for the binary mixture and fitted using Redlich-Kister polynomial equation. Calorimetric excess chemical potential is also estimated through these physicochemical properties using 3-parameter Margules, Porter, Wilson and Van Laar equations at T=308.15K. In addition, non-linearity parameter using two different models is also evaluated along with certain molecular properties. Lastly, an attempt has been made to understand the interaction behavior between the two liquids in the mixture using IR spectroscopy. In addition, analysis of V_m^E data of the present mixture was done through the Prigogine-Flory-Patterson (PFP) theory.

2. Experimental

2.1. Materials

The ionic liquid, [Bmim][NTf₂] (CAS174899-83-3) with purity 0.99 in mass fraction used in this work. It was purchased from Iolitec GmbH (Germany), while DMC (CAS616-38-6) with purity 0.995 in mass fraction was supplied by Sigma Aldrich. The chemicals used in the present investigation were purified by the methods described in literature [39,40]. The water

content in investigated IL and DMC was determined using a Karl Fisher titrator (Mettler, 890Titrando). Before any measurements, all samples were dried for at least 72h under a vacuum (0.1Pa) and moderate temperature (beginning at room temperature and increasing it gradually over a 6 h period up to 333K). The water content of all the samples were further checked and found to be in the range of less than 150 ppm, a value much lower than the original pre-evacuation analysis, which typically showed values in the range of less than 210×10^{-6} . DMC is further purified by distillation. List of chemicals with details of Provenance, CAS number, and mass fraction purity are given in **Table 1**. The purities were verified by comparing the measured density, speed of sound and refractive index of the pure liquids with the literature at atmospheric pressure are given in **Table 2**. Figures S1–S6 of the supplementary material represent comparison of pure values of densities, speeds of sound and refractive indices of [Bmim][NTf₂] and DMC of this work with the reported literature [31,32,35,38,41–44,46–66]. The experimental refractive index data show much discrepancy with the literature. With regards to refractive index of the [Bmim][NTf₂], our data show deviation of -0.05 %, -0.04% and -0.11% with the data of Krishna *et al.* [38], Montalban *et al.* [54] at 303.15 K and Tariq *et al.* [55] at 313.15 K respectively. Moreover, the refractive index data of DMC have deviations of +0.05%, +0.06% with the data of Rodriguez [62], Shin *et al.* [43] and -0.03% of Moosavi *et al.* [66] at 303.15 K and -0.23 % from Pal *et al.* [65] at 308.15 K respectively. The observed deviations may be due to variation of percentage of purity and instruments. We used latest version of Anton Paar DSA 5000M/ Anton Paar Dr Krenchen Abbatemat (WR-HT) having automatic viscosity corrector giving high accurate values. Further, our samples, [Bmim][NTf₂] and DMC have 99% and 99.5% purity respectively. We have taken utmost care to remove water content.

2.2 Apparatus and procedure

2.2.1. Sample preparation

All samples are freshly prepared in amber colour glass vials with screw caps having PFE septa, and are securely sealed with parafilm to prevent absorption of moisture from the atmosphere, and is then stirred for more than 30 min to ensure total dissolution of the mixtures. Samples are taken from the vials with a syringe through the PFE septum. Samples are prepared by weighing

with a precision of ± 0.01 mg, using a Sartorius electronic balance (CPA225D). The uncertainty of the resulting mole fractions of the mixtures was estimated as being $\pm 5 \times 10^{-4}$.

2.2.2. Measurement of density and speed of sound

Densities and speed of sound are measured with an Anton Paar DSA-5000M vibrating tube density and sound velocity meter. The density meter is calibrated with doubly distilled degassed water, and with dry air at atmospheric pressure. The temperature of the apparatus is controlled to within ± 0.01 K by a built-in Peltier device. Measured density and speed of sound values (at frequency approximately 3 MHz) are precise to $5 \times 10^{-3} \text{ kg} \cdot \text{m}^{-3}$ and $5 \times 10^{-1} \text{ m} \cdot \text{s}^{-1}$ respectively. The standard uncertainties associated with the measurements of temperature, density and speed of sound are estimated to be ± 0.01 K, $1 \text{ kg} \cdot \text{m}^{-3}$ and $\pm 0.5 \text{ m} \cdot \text{s}^{-1}$ respectively.

2.2.3 Measurement of refractive index

The refractive indices are determined using an automatic refractometer (Anton Paar Dr Krenchen Abbemat (WR-HT)) which has also a temperature controller that keeps the samples at working temperature. The uncertainties in the temperature and refractive index values are $\pm 0.01 \text{ K}$ and $\pm 5 \times 10^{-4}$ respectively. The apparatus is calibrated by measuring the refractive index of Millipore quality water and tetrachloroethylene (supplied by the company) before each series of measurements according to manual instructions. The calibration is checked with pure liquids by known refractive index.

2.2.4 Measurement of infrared spectra

Infrared transmittance is measured by using Shimadzu Fourier transform infrared (FT-IR) spectrometer (IR Affinity-1S) equipped with attenuated total reflectance (ATR) accessories. The spectral region is $(650-4000) \text{ cm}^{-1}$ with resolution of 2 cm^{-1} and 100 scans. At least five repeated measurements are performed for each sample.

3. Results and Discussion

The experimentally measured density (ρ), speed of sound (u) and refractive index (n_D) for the binary mixture of [Bmim][NTf₂] with DMC over the region of complete miscibility as a function of temperature between (303.15-323.15) K in steps of 5 K under atmospheric pressure are given in the **Table 3**. The changes in values of ρ , u and n_D with respect to temperature and mole fraction are linear and non-linear respectively. This trend specifies that molecular interactions definitely exist at all temperature between liquids in study. The excess and deviation

parameters are calculated from the experimental data according to well-known thermodynamic expressions given below.

The excess molar volume is given by

$$V_m^E = \frac{x_1 M_1 + x_2 M_2}{\rho} - \left(\frac{x_1 M_1}{\rho_1} + \frac{x_2 M_2}{\rho_2} \right) \quad (1)$$

where, M_1 & M_2 represent molar mass, x_1 & x_2 the mole fractions of [Bmim][NTf₂] and DMC respectively, while ρ_1 , ρ_2 & ρ the densities of [Bmim][NTf₂], DMC and the mixture respectively.

The isentropic compressibility, κ_s , is computed directly from the measured values of speed of sound and density using the Newton-Laplace equation

$$\kappa_s = -\frac{1}{V_m} \left(\frac{\partial V_m}{\partial P} \right)_s = \left(\frac{1}{\rho u^2} \right) = \left(\frac{V_m}{M u^2} \right) \quad (2)$$

Excess isentropic compressibility is given by

$$\kappa_s^E = \kappa_s - \kappa_s^{id} \quad (3)$$

where, κ_s , is the isentropic compressibility and κ_s^{id} , is the isentropic compressibility of the ideal mixture, which is calculated in the manner as suggested by Benson and Kiyohara [67].

$$\kappa_s^{id} = \sum_{i=1}^2 \phi_i \left[\kappa_{s,i} + \frac{T V_i \alpha_i^2}{C_{p,i}} \right] - \left\{ T \frac{\left(\sum_{i=1}^2 x_i V_i \right) \left(\sum_{i=1}^2 \phi_i \alpha_i \right)^2}{\left(\sum_{i=1}^2 x_i C_{p,i} \right)} \right\} \quad (4)$$

where, ϕ_i , is the volume fraction of the i^{th} component and is given by, $\phi_i = \frac{x_i V_i}{\sum_{i=1}^2 x_i V_i}$, T is the

temperature, $\kappa_{s,i}$ is the isentropic compressibility, V_i is the molar volume, α_i is the isobaric thermal expansion coefficient and $C_{p,i}$ is heat capacity of the i^{th} component.

Free length is given by

$$L_f = \kappa_j (\kappa_s)^{1/2} \quad (5)$$

where, κ_j is the temperature dependent Jacobson's constant which is equal to $\kappa_j = (93.875 + 0.375T) 10^{-8}$

The excess intermolecular free length is given by

$$L_f^E = L_f - L_f^{id} = \kappa_j (\kappa_s)^{1/2} - \kappa_j (\kappa_s^{id})^{1/2} \quad (6)$$

The excess speeds of sound, u^E is estimated in binary and ternary mixtures using the following expression [68].

$$u^E = u - u^{id} = u - (\rho^{id} k_s^{id})^{-1/2} \quad (7)$$

$$\text{where } \rho^{id} = \sum_{i=1}^2 \phi_i \rho_i$$

Isobaric thermal expansion coefficient, α_p , of the pure components is calculated from the measured densities by the relation,

$$\alpha_p = \frac{1}{V_m} \left(\frac{\partial V_m}{\partial T} \right)_p = -\frac{1}{\rho} \left(\frac{\partial \rho}{\partial T} \right)_p = -\left(\frac{\partial \ln \rho}{\partial T} \right) \quad (8)$$

The values of α_p are derived by taking differentiation of second order polynomial fit [69] between density and temperature ($R^2 > 0.999$).

Excess isobaric thermal expansion coefficient, α_p^E is calculated from the following equation

$$\alpha_p^E = \alpha_p - \alpha_p^{id} = \frac{\left(\frac{\partial V_m^E}{\partial T} \right)_p - V_m^E \alpha_p^{id}}{V_m^{id} + V_m^E} \quad (9)$$

$$\text{where, } \alpha_p^{id} = \sum_{i=1}^2 \phi_i \alpha_{p,i}^*$$

The dependence of the excess molar enthalpy of mixing with pressure at fixed temperature $\left(\frac{\partial H_m^E}{\partial P} \right)_T$ can be derived indirectly from accurate measurement of V_m^E , as a function

of the temperature and composition by application of the following exact thermodynamic expression

$$\left(\frac{\partial H_m^E}{\partial P}\right)_T = V_m^E - T \left(\frac{\partial V_m^E}{\partial T}\right)_P \quad (10)$$

If the difference between the refractive indices of the two components is small then deviation in refractive index of binary mixtures containing ILs

$$\Delta \phi n_D = n_D - n_D^{id} \quad (11)$$

$$n_D^{id} = \phi_1 n_{D,1} + \phi_2 n_{D,2}$$

The excess/deviation properties are fitted to a Redlich-Kister polynomial equation given by

$$Y^E = x_1 x_2 \sum_{i=0}^j A_i (x_1 - x_2)^i \quad (12)$$

Where $Y^E = V_m^E, \kappa_s^E, L_f^E, u^E, \alpha_P^E, \Delta \phi n_D, \left(\frac{\partial V_m^E}{\partial T}\right)_P$ and $\left(\frac{\partial H_m^E}{\partial P}\right)_T$. x_1 and x_2 are the mole fraction of [Bmim][NTf₂] and DMC respectively. Further, A_i are the adjustable parameters of the function; and are determined using the least square method. In the present investigation ‘ i ’ values are taken from 0 to 4. The corresponding standard deviations $\sigma(Y^E)$ are calculated using the following expression.

$$\sigma(Y^E) = \left[\frac{\sum (Y_{\text{exp}}^E - Y_{\text{cal}}^E)^2}{(m - n)} \right]^{1/2} \quad (13)$$

where ‘ m ’ is the total number of experimental points and ‘ n ’ is the number of coefficients in equation (12). The Redlich-Kister polynomial coefficients and corresponding standard deviations are presented in **Table 4**.

The variations as observed in these excess/deviation parameters indicate the strength of interactions that exist between the component molecules of the binary mixture under study and their further dependence on the composition, molecular size, shape and temperature. The effects which influence these thermodynamic functions may be the resultant contribution from several opposing effects, namely chemical, structural, and physical [70,71]. The chemical or specific

interactions include the formation of hydrogen bonding between component molecules, charge-transfer complexes. The structural contributions arise from several effects such as interstitial accommodation and geometrical fitting of one component into another. Excess molar volumes for the binary mixture of [Bmim][NTf₂] with DMC as a function of composition from $T = (303.15-323.15)$ K are shown in **Figure 1**. Excess molar volumes are found to be negative in the entire composition at all temperatures. The variations of excess molar volumes are found to be negative in the whole composition range at all temperatures which may be credited to the hydrogen bonding between solute and solvent molecules and also favourable fitting of smaller DMC molecules (at $T=303.15\text{K}$, $V_m=85.24 \times 10^{-6} \text{ m}^3\cdot\text{mol}^{-1}$) into the voids created by larger [Bmim][NTf₂] molecules (at $T=303.15\text{K}$, $V_m=293.48 \times 10^{-6} \text{ m}^3\cdot\text{mol}^{-1}$) is definitely contributing to interactions. The similar variations in V_m^E values are also observed for the rest of studied temperatures. Moreover, the variation of V_m^E for the present system as a function of temperature becomes more negative with rise in temperature. This is because of the fact that, more favourable fitting of smaller DMC molecules into the voids created by larger IL molecules, thereby, shrinkage of the volume of the mixture to a larger extent, resulting in more negative V_m^E values with rise in temperature. Therefore, order of strength of interaction enhances with rise in temperature.

The existing molecular interactions in the current binary system are properly reflected on the properties of partial molar volumes of the constituent molecules. Partial molar volume is the contribution that a component of a mixture makes to the total volume of the solution. Therefore, the partial molar volume is a function of mixture composition. The partial molar volumes $\bar{V}_{m,1}$ of component 1 ([Bmim][NTf₂]) and $\bar{V}_{m,2}$ of component 2 (DMC) in the mixtures over the whole composition range have been computed using the following relationships.

$$\bar{V}_{m,1} = V_m^E + V_1^* + x_2 \left(\frac{\partial V_m^E}{\partial x_1} \right)_{T,P} \quad (14)$$

$$\bar{V}_{m,2} = V_m^E + V_2^* - x_1 \left(\frac{\partial V_m^E}{\partial x_1} \right)_{T,P} \quad (15)$$

where V_1^* and V_2^* are the molar volumes of pure components of [Bmim][NTf₂] and DMC respectively. The derivatives in the above equations are obtained by differentiating Redlich-Kister eqn. (14) that leads to the following equations for $\bar{V}_{m,1}$ and $\bar{V}_{m,2}$.

$$\bar{V}_{m,1} = V_1^* + x_2^2 \sum_{i=0}^4 A_i (x_1 - x_2)^i - 2x_1 x_2^2 \sum_{i=1}^4 A_i (i) (x_1 - x_2)^{i-1} \quad (16)$$

$$\bar{V}_{m,2} = V_2^* + x_1^2 \sum_{i=0}^4 A_i (x_1 - x_2)^i + 2x_2 x_1^2 \sum_{i=1}^4 A_i (i) (x_1 - x_2)^{i-1} \quad (17)$$

using the above equations $\bar{V}_{m,1}^E$ and $\bar{V}_{m,2}^E$ have been calculated using,

$$\bar{V}_{m,1}^E = \bar{V}_{m,1} - V_1^* \quad (18)$$

$$\bar{V}_{m,2}^E = \bar{V}_{m,2} - V_2^* \quad (19)$$

The calculated values of $\bar{V}_{m,1}$ and $\bar{V}_{m,2}$ for the studied binary system are represented in **Table 5**. On visualizing the values of $\bar{V}_{m,1}$ and $\bar{V}_{m,2}$ for the two components in the mixtures (**Table 5**), it is evident that the values are lower than their individual molar volumes in the pure state, which reveals contraction of volume occurs on mixing [Bmim][NTf₂] with DMC at all examined temperatures. **Figure 2** and **Figure 3** represent the disparity of excess partial molar volumes of $\bar{V}_{m,1}^E$ ([Bmim][NTf₂]) and $\bar{V}_{m,2}^E$ (DMC) respectively in the binary mixture at $T = (303.15, 308.15, 313.15, 318.15 \text{ and } 323.15)$ K. The **Figure 2** and **Figure 3** not only show the existence of strong forces between the unlike molecules but also supports the inferences drawn from excess molar volume.

The excess partial molar volumes at infinite dilution of component 1 ($\bar{V}_{m,1}^{E,\infty}$) and component 2 ($\bar{V}_{m,2}^{E,\infty}$) have been calculated using

$$\bar{V}_{m,1}^{E,\infty} = A_0 - A_1 + A_2 - A_3 + \dots = \bar{V}_{m,2}^\infty - V_2^* \quad (20)$$

$$\bar{V}_{m,2}^{E,\infty} = A_0 + A_1 + A_2 + A_3 + \dots = \bar{V}_{m,1}^\infty - V_1^* \quad (21)$$

The partial molar volumes ($\bar{V}_{m,1}^\infty, \bar{V}_{m,2}^\infty$) and excess partial molar volumes at infinite dilution ($\bar{V}_{m,1}^{E,\infty}, \bar{V}_{m,2}^{E,\infty}$) of [Bmim][NTf₂] and DMC are calculated using the equations (18-21). The pertinent

data of $\bar{V}_{m,1}^{\infty}$, $\bar{V}_{m,2}^{\infty}$ and $\bar{V}_{m,1}^{E,\infty}$, $\bar{V}_{m,2}^{E,\infty}$ is presented in **Table 6** at $T = (303.15, 308.15, 313.15, 318.15$ and $323.15)$ K. The values of $\bar{V}_{m,1}^{E,\infty}$ and $\bar{V}_{m,2}^{E,\infty}$ are found to be negative and become more negative with increase of temperature. This indicates that the association effect is greater than the dissociation effect for both the components in the present system. The excess partial molar volumes at infinite dilution for [Bmim][NTf₂] ($\bar{V}_{m,1}^{E,\infty}$) are more negative than those of DMC ($\bar{V}_{m,2}^{E,\infty}$) at all studied temperatures. This is because for more concentrated DMC solution, no hydrogen bonds exist among DMC molecules. Hence we conclude that strong interactions increase among the unlike molecules of the mixtures with increase in temperature [72]. These are noticed in the case of V_m^E values in the binary system which are well reproduced from the evaluated properties of partial molar volumes at infinite dilution as well as at all investigated temperatures.

In **Figure 4**, the κ_s^E values for [Bmim][NTf₂]+DMC are negative over the whole composition range at all investigated temperatures. The negative κ_s^E values attributed to the strong attractive interactions between the molecules of the components [73]. This supports the inference drawn from V_m^E . The intermolecular free length indicates closer approach of unlike molecules. The trends of L_f^E values (**Figure 5**) are negative at all investigated temperatures. The negative values of L_f^E are generally observed due to the dominance of specific interactions between unlike molecules in the liquid mixture and also due to the structural readjustments in the liquid mixture towards a less compressible phase of fluid and closer packing of molecules [74]. **Figure 6** shows that the u^E values are positive for the system over the entire range of composition at all temperatures studied. Positive deviations indicate the increasing strength of interaction between component molecules of binary liquid mixtures. In general, strong interactions among the components of a mixture lead to the formation of molecular aggregates and more compact structures; then sound will travel faster through the mixture [75]. According to Ali *et al.* [76], more positive values mean much more strong interactions between the molecules.

The refractive indices (n_D) for the binary mixtures at the studied temperatures over the whole composition range are given in **Table 3** which increases with increase in the concentration of the ILs in the mixture and decreases as the temperature increases for a particular concentration

of [Bmim][NTf₂]. The values of $\Delta_\phi n_D$ are positive over the studied range of composition for the binary mixtures (**Figure 7**) which may be attributed to the non-availability of the free volume in the mixture in comparison with the ideal mixtures. As the mole fraction of the [Bmim][NTf₂] increases, V_m^E becomes more negative because the free space available decreases in the mixtures and speed of the light travel with lesser velocity than that in the ideal mixtures [77,78]. This gives increase in refractive index (n_D) causing $\Delta_\phi n_D$ positive. Further, as temperature increases, V_m^E found to become more negative consequently $\Delta_\phi n_D$ become more positive. Thus the inference of $\Delta_\phi n_D$ also supports the increase of strength of strong interactions with increase in temperature.

The negative values of α_p^E are due to strong interactions between solute and solvent molecules [79]. **Figure 8** shows negative values of α_p^E in the whole composition range and at all investigated temperatures for the binary mixture in study. This further supports the existence of strong interactions between the constituent molecules in binary liquid solution. In **Figure 9** and **Figure 10**, the values of excess functions $\left(\frac{\partial V_m^E}{\partial T}\right)_P$ and $\left(\frac{\partial H_m^E}{\partial P}\right)_T$ are plotted against mole fraction of [Bmim][NTf₂]. The variation of $\left(\frac{\partial V_m^E}{\partial T}\right)_P$ and $\left(\frac{\partial H_m^E}{\partial P}\right)_T$ is similar with the mole fraction and temperature but with opposite sign. The negative values of $\left(\frac{\partial V_m^E}{\partial T}\right)_P$ for the studied mixture may be due to strong interactions existing between the unlike molecules of the mixture [80]. The isothermal pressure coefficient of excess molar enthalpy $\left(\frac{\partial H_m^E}{\partial P}\right)_T$ has positive values in the whole composition range. This reflects increase in attraction forces between two components of this mixture by increasing pressure. Hence, contraction in the volume of the mixture is still possible by increasing pressure [81].

Phase equilibria are essential for chemical separation process design. The imperfectness of the liquid phase is accounted by liquid-phase excess chemical potential by way of thermodynamic models. Experimental data are frequently unavailable over the range of conditions of interest; for this reason, the required data must be estimated using one of a variety

of approaches. In this paper an attempt has been made to predict excess chemical potentials using 3-parameter Margules (Standard error: 0.0113), Porter (Standard error: 0.0904), Wilson (Standard error: 0.0404) and Van Laar (Standard error: 0.0340) equations at $T=308.15$ K rather calorimetric method. For the present scenario, estimated excess chemical potentials using various theories are plotted in **Figure 11** with composition of [Bmim][NTf₂] at $T=308.15$ K. Further, it is worthy to note that the curved lines emanated from four theories show non-ideal deviation from the ideal case [82] supporting the presence of molecular interactions between the hetero molecules in study.

The non-linearity parameter (B/A) is a gauge of the non-linearity of the equation of state for a fluid. It shows a significant position in acoustics, from underwater acoustics to biology and medicine. The non-linearity parameter indicates deformation of a finite amplitude wave spreading in the liquid. Further, it can be correlated to the molecular dynamics of the medium and it can bestow information concerning structural properties of medium, internal pressure, clustering, and inter-molecular spacing, etc. Significance of the B/A parameter rises with the advancement of high-pressure technologies of food processing and preservation. Therefore, an effort has been made to assess the values of molecular properties of the liquid mixtures using non-linearity parameter (B/A) values from semi empirical relations proposed by Hartmann – Balizar (H&B) [83] and Ballou [84] with the use of Sehgal's relations [85]. The microscopic parameters pertinent to the binary liquid system like cohesive energy (ΔA), Van der Waal's constants (a & b) and the distance of closest approach (d) are estimated and tabulated in **Table 7**. The relevant equations pertinent to excess chemical potentials are provided in the supplementary material. It is to be noted that excess values of (B/A) are found to be negative at all temperatures. Negative/positive values of (B/A)^E indicate the presence of strong/relatively weak interactions between unlike molecules [86] respectively. Thus negative values of (B/A)^E also supports the existence of strong interactions in the present binary system under study.

3.1. Infrared spectral studies

The existence of strong interactions in the system which were drawn from the above inferences of derived excess/deviation parameters are well supported by IR spectral studies. The unique properties of imidazolium cations are found in their electronic structure. The electronic structure of imidazolium cations (**Figure 12**) contains delocalized 3-center-4-electron

configuration across the N_1 - C_2 - N_3 moiety, a double bond between C_4 and C_5 at the opposite side of the ring, and a weak delocalization in the central region [87]. The hydrogen in C_2 -H is more acidic than C_4 -H, and C_5 -H due to the electron deficiency in the $C=N$ bond. The resultant acidity of the hydrogen atoms is key to understand the properties of these ionic liquids. The hydrogen on the C_2 carbon (C_2 -H) has been shown to bind typically with solute molecules [88, 89].

In order to study the effects of molecular interactions, infrared absorbance are recorded from 650 cm^{-1} to 4000 cm^{-1} (**Figure 13 and Table 8**). In $[Bmim]^+$ cation, the C-H stretching region from $(2800\text{ to }3200)\text{ cm}^{-1}$ is investigated. For $[Bmim][NTf_2]$, the signals in this region can be separated into two parts: signals between 3000 cm^{-1} and 3200 cm^{-1} can be attributed to C-H vibrational modes mainly arising from the aromatic imidazolium ring, from C_2 -H and $C_{4,5}$ -H stretching frequencies [90]. The signals between 2800 cm^{-1} and 3000 cm^{-1} are due to aliphatic C-H groups in the methyl and butyl moieties [91-93]. The C_2 -H vibrational frequency (3120.7 cm^{-1}) is shifted to lower frequencies by about 36.5 cm^{-1} when compared to the C_4 -H and C_5 -H stretches (3157.2 cm^{-1}) because of its stronger acidic character. In $[Bmim][NTf_2]$, there exist hydrogen bond between aromatic C-H hydrogen's of the cation and oxygen, fluorine atoms of the anion [94]. In the present mixtures, C_2 -H and $C_{4,5}$ -H stretching frequencies of the cation and SO_2 Sym Stretch, CF_3 Sym Stretch of the anion are analysed where there is no overlap from peaks of DMC. As mole fraction of IL (x_1) changes from 1.0000 to 0.7006, not very much change in the frequencies indicating the existence of ionic clusters. Further, in the region between $x_1=0.7006$ and $x_1=0.4158$, the significant change in $[NTf_2]^-$ ion frequencies indicated the formation of ion pairs from clusters. Furthermore, in DMC rich region ($x_1<0.4158$), complete solvation of individual ions take place. There is a slight red shift in C_2 -H and $C_{4,5}$ -H stretching frequencies indicating the formation of hydrogen bond between $[Bmim]^+$ and DMC. Simultaneously, a clear blue shift in SO_2 Sym Stretch, CF_3 Sym Stretch frequencies is observed because of the breakup of hydrogen bond between cation and anion of the ionic liquid. The shifts are predominant at DMC rich region.

By examining ATR-FTIR, it can be accomplished that hydrogen bonds exist extensively in such systems which play a key role towards the miscibility and stability of the $[Bmim][NTf_2]$ +DMC binary system. Additionally, the hydrogen bonding interactions are also accountable in the present system to get complete miscibility and solvation. Hence, it can be

assumed that the hydrogen bonds between the ionic liquid [Bmim][NTf₂] and DMC are also responsible to make a remarkable contraction in the volume of the mixture.

3.2. Prigogine-Flory-Patterson statistical theory for excess molar volume V_m^E

The Prigogine-Flory-Patterson (PFP) theory may be used to analyse and correlate the experimental excess molar volumes of binary mixtures [95-98]. We have correlated V_m^E of presently studied binary mixture using PFP theory over the entire range of mole fractions at $T = (303.15-323.15)$ K. The PFP theory considered V_m^E for three different contributions [99]: (i) interaction contribution V_{int}^E , which is associated with intermolecular specific interaction with sign of H_m^E (ii) free volume contribution V_{fv}^E , which is associated with reduced volume to reduced temperature ratio with negative sign (iii) internal pressure contribution, $V_{p^*}^E$, which is associated with breaking of IL structure with introduction of molecular organic solvents and changes in reduced volume of components with positive or negative sign. The detailed equations of PFP theory are given in supplementary material.

The pure components parameters for the PFP theory are included in **Table 9**. **Figure 14** indicates the composition dependence of values calculated from PFP theory for [Bmim][NTf₂]+DMC mixture compared with experimental at 303.15K. The Flory contact interaction parameter χ_{12} , the only adjustable parameter, needed in the PFP theory was obtained by experimental V_m^E values in absence of the experimental excess molar enthalpy (H_m^E). The Flory contact interaction parameter χ_{12} was found to be negative for all the investigated temperatures. The values of three contributions: V_{int}^E , V_{fv}^E and $V_{p^*}^E$, to V_m^E (PFP) at equimolar composition are summarized in **Table 10**. The first term V_{int}^E is negative which suggests that the strong interactions take place in the binary mixture. The interactional contributions are negative at all calculated temperatures. The second term V_{fv}^E was found to be negative for the system studied (**Table 10**) as V_{fv}^E is proportional to $-(\tilde{v}_1 - \tilde{v}_2)^2$ [96]. The magnitude of negative values for V_{fv}^E depends upon difference in Flory's reduced volumes of involved components. Negative values of V_{fv}^E increases in magnitude as the temperature increases which shows that as the temperature increases, more free volume in the [Bmim][NTf₂] becomes available to accommodate the smaller DMC molecules which resulted in more negative V_m^E . The third term,

i.e. characteristic pressure $V_{P^*}^E$, the P^* effect which depends on the relative cohesive energy of the expanded and less expanded component is found to be positive at all investigated temperatures. It is proportional to $(\tilde{V}_1 - \tilde{V}_2)(P_1^* - P_2^*)$ and can have both the negative and positive sign depending upon the magnitude of P_i^* and \tilde{V}_i^* of unlike components [104]. For the system [Bmim][NTf₂] + DMC, $V_{P^*}^E$ is positive which is related to the structure-braking effect of the DMC on the electrostatic interactions between the ions of [Bmim][NTf₂] and so the DMC molecules can be placed around the [Bmim]⁺ and [NTf₂]⁻ ions [96,104]. In the present system, V_{int}^E and V_{fv}^E were found to be negative while $V_{P^*}^E$ was found to be positive which shows that the interaction and free volume contributions are responsible for the overall strong interactions between solute and solvent molecules. From **Figure 14**, the V_m^E values calculated from PFP theory are in good agreement with the experimental values particularly at IL rich region. We can conclude that, it is possible to explain the volumetric behavior of [Bmim][NTf₂] + DMC binary mixture by the application of the PFP theory quite successfully.

4. Conclusions

Densities, ultrasonic speed of sounds and refractive indices for binary liquids of [Bmim][NTf₂] with DMC have been measured experimentally at atmospheric pressure over the entire composition range at temperature 303.15 K, 308.15 K, 313.15 K, 318.15 K and 323.15 K. From the experimental data, excess/ deviation properties such as V_m^E , κ_S^E , L_f^E , u^E , α_p^E and $\Delta_\phi n_D$ have been evaluated. The excess and deviation parameters have been fitted to Redlich-Kister type polynomial and also corresponding standard deviations have been computed. In the present binary liquid systems of [Bmim][NTf₂] with DMC, the observed excess values clearly reflecting the dominance of strong attractive forces. The order of strong interactions follows (303.15 < 308.15 < 313.15 < 318.15 < 323.15) K. The observed lower partial molar volumes in the liquid mixture when compared to the molar volumes of respective pure components also support the existence of strong interactions in the system. An attempt for the estimation of excess chemical potentials is made using 3-parameter Margules, Porter, Wilson and Van Laar at T=308.15 K. Non-linear parameter (B/A) is evaluated using semi empirical relations and certain molecular properties are calculated from Sehgal's equations. Negative values of $(B/A)^E$ also support the existence of strong interaction between the components of mixture at all temperatures. The IR

spectral studies also supported the presence of strong interaction between molecules in study. PFP theory was able to explain the volumetric behaviour of the system quite successfully.

References

- [1] T.L.Greaves, C.J.Drummond, *Chem.rev.*, 115 (2015) 11379-11448.
- [2] F.Guo, S.Zhang, J.Wang, B.Teng, T.Zhang, M.Fan, *Curr. Org.Chem.* 19 (2015) 455-468.
- [3] A.A.Shamsuri, R.Daik, *Rev. Adv.Mat.Sci.* 40 (2015) 45-59.
- [4] C. Comminges, R. Barhdadi, M. Laurent, M. Troupel, *J. Chem. Eng. Data* 2006, 51, 680–685.
- [5] M. D. Bhatt, C. O'Dwyer, *Phys. Chem. Chem. Phys.* 2015, 17, 4799–4844.
- [6] C. J. Allen, S. Mukerjee, E. J. Plichta, M. A. Hendrickson, K. M. Abraham, *J. Phys. Chem. Lett.* 2011, 2, 2420–2424.
- [7] S. Park, R.J. Kazlauskas, *Curr. Opin. Biotechnol.* 14 (2003) 432.
- [8] M. Sureshkumar, C.-K. Lee, *J. Mol. Catal. B Enzym.* 60 (2009) 1.
- [9] M. Moniruzzaman, K. Nakashima, N. Kamiya, M. Goto, *Biochem. Eng. J.* 48 (2010) 295.
- [10] J.V. Rodrigues, D. Ruivo, A. Rodríguez, F.J. Deive, J.M.S.S. Esperança, I.M. Marrucho, C.M. Gomes, L.P.N. Rebelo, *Green Chem* 16 (2014) 4520.
- [11] M.N. da Graça, J.M.R. da Silva, J.C. da Silva, M.M. Alves, *J. Mol. Catal. B Enzym.* 112 (2015) 1-8.
- [12] P. Lozano, T. Diego, D. Carrie, M. Vaultier, J. Iborra, *Chem.Comm.* 7 (2002) 692–693.
- [13] M.B. Turner, S.K. Spear, J.D. Holbrey, R.D. Rogers, *Biomacromolecules* 5(2004)1379–1384.
- [14] M.B. Turner, S.K. Spear, J.D. Holbrey, D.T. Daly, R.D. Rogers, *Biomacromolecules* 6 (2005) 2497–2502.
- [15] S.S.Y. Tan, D.R. MacFarlane, J. Upfal, Edye LA, W.O. Doherty, A.F. Patti, J.M. Pringle, J.L. Scott, *Green Chem* 11 (2009) 339–345.
- [16] M. Gericke, T. Liebert, T. Heinze, *Macromol Biosci.* 9 (2009) 343–353.
- [17] M. Gericke, J. Schaller, T. Liebert, P. Fardim, F. Meister, T. Heinze, *Carbohydr Polym.* 89 (2012) 526–536
- [18] C. Yao, J.L. Anderson, *Anal. Bioanal. Chem.* 395 (2009) 1491–502.

- [19] D. Hameister, S. Illner, C. Vogel, D. Michalik, U. Kragl, *Sep. Purif. Technol.* 132 (2014) 438-445.
- [20] D. Betz, A. Raith, M. Cokoja, F.E. Kuehn, *ChemSusChem*. 3 (2010) 559-562.
- [21] T.D. Ho, P.M. Yehl, N.P. Chetwyn, J. Wang, J.L Anderson, Q. Zhong, *J. Chromatogr. A*, 1361 (2014) 217-228.
- [22] A. Kokorin, *Ionic liquids: applications and perspectives*, InTech (2011).
- [23] M.H. Mabaso, G.G. Redhi, K.G. Moodley, *S. African J.Chem.*65 (2012) 145-149.
- [24] J. Barthel, R. Neueder, H. Poepke, H. Wittmann, *J. Solution Chem.* 28 (1999) 489-503.
- [25] A. Laheear, H Kurig, A. Janes, E. Lust, *Electrochim. Acta.* 54 (2009) 4587-4594.
- [26] F. Rivetti, in: P.T. Anastas, P. Tundo (Eds.), *Green Chemistry: Challenging Perspectives*, Oxford University Press, Oxford (2001) 201.
- [27] G. Gerbaz, G. Fisicaro, in: R.L. Shubkin (Ed.), *Synthetic Lubricants and High Performance Functional Fluids*, Marshall Dekker, New York (1993) 229.
- [28] B. Scrosati, *Nanocomposite polymer electrolytes for lithium batteries*, *Chim. Ind. (Milan)* 79 (1997) 463.
- [29] E. Alfonsina, Andreatta, A. Alberto, E. Rodil, A. Soto, *J. Solution Chem.* 39 (2010) 371-383
- [30] R. Zarrougui, M. Dhahbi, D. Lemordant, *J. Solution Chem.* 39 (2010) 921-942.
- [31] E. Widowati, M. J Lee, *J. Chem. Thermodyn.* 63 (2013) 95-101.
- [32] M. Vranes, N. Zec, A. Tot, S. A. Papovic, S. Dozic, S.Gadzuric, *J. Chem. Thermodyn.* 68 (2014) 98-108.
- [33] M. Geppert-Rybczynska, M. Sitarek, *J. Chem. Eng. Data* 59 (2014) 1213-1224.
- [34] M. Vranes, S. AnaPapovic, A. Tot, N. Zec, S.Gadzuric, *J. Chem. Thermodyn.* 76 (2014) 161-171.
- [35] R. Salinas, J. Pla-Franco, E. Lladosa, Juan B. Monto, *J. Chem. Eng. Data* 60(2015) 525-540.
- [36] J. Jacquemin, P. Husson, A.A. Padua, V. Majer, *Green Chem.* 8 (2006) 172-180.
- [37] M. AzlanKassim, N. AsrinaSairi, R. Yusoff, A. Ramalingam, Y. Alias, M. K. Aroua, *Thermochim. Acta* 639 (2016) 130-147
- [38] T. Srinivasa Krishna, Anil K. Nainb, S. Chentilnathc, D. Punyaseshadud, B. Munibhadrayyae, J. *Chem. Thermodyn.* 101 (2016) 103-114.

- [39] W. L. Armarego, C. L. L. Chai, Purification of laboratory chemicals. Butterworth-Heinemann (2013).
- [40] E. Scholz, Karlfisher titration, Springer-Verlag: Berlin (1984).
- [41] R. Ren, Y. Zuo, Q. Zhou, H. Zhang, S. Zhang, Density, J. Chem. Eng. Data 56 (2010) 27-30.
- [42] A. B. Pereiro, A. Rodriguez, J. Canosa, J. Tojo, J. Chem. Eng. Data 2004, 49, 1392-1399
- [43] S. H. Shin, I. Y. Jeong, Y. S. Jeong, S. J. Park, Fluid Phase Equilib. 376 (2014) 105-110.
- [44] J. Troncoso, C.A. Cerdeirin, Y.A. Sanmamed, L. Roman, L. Paulo, N. Rebelo, J. Chem. Eng. Data 51 (2006) 1856-1859.
- [45] B.R.Arbad, M.K.Lande, N. N. Wankhede, D.S.Wankhede, J. Chem. Eng. Data 51 (2006) 68-72.
- [46] R. Hamidova, I. Kul, J. Safarov, A. Shahverdiyev, E. Hassel, 2015. Braz. J. Chem. Eng. 32 (2015) .303-316.
- [47] Y. Hiraga, A. Kato, Y. Sato, R.L. Smith Jr, J. Chem. Eng. Data, 60 (2015).876-885.
- [48] M. Kanakubo, K.R. Harris, J. Chem. Eng. Data. 60 (2015) 1408-1418.
- [49] C.A.N. de Castro, E. Langa, A.L. Morais, M.L.M. Lopes, M.J. Lourenço, F.J. Santos, M.S.C. Santos, J.N.C. Lopes, H.I. Veiga, M. Macatrão, J.M. Esperança, Fluid Phase Equilib., 294 (2010).157-179.
- [50] J. Jacquemin, P. Husson, V. Mayer, I. Cibulka, J. Chem. Eng. Data, 52 (2007) 2204-2211.
- [51] M.R. Currás, P. Husson, A.A. Pádua, M.F. Costa Gomes, J. García, Ind.Eng.Chem. Res., 53 (2014) 10791-10802.
- [52] R.G. De Azevedo, J.M.S.S. Esperanca, J. Szydlowski, Z.P. Visak, P.F. Pires, H.J.R. Guedes, L.P.N. Rebelo, J. Chem. Thermodyn., 37 (2005) 888-899.
- [53] N.I. Malek, S.P. Ijardar, J. Chem. Thermodyn., 93 (2016) 75-85.
- [54] M.G. Montalban, C.L. Bolivar, F.G. Díaz Baños, G. Villora, J. Chem. Eng. Data, 60 (2015) 1986-1996.
- [55] M. Tariq, P.A.S. Forte, M.C. Gomes, J.C. Lopes, L.P.N. Rebelo, J. Chem. Thermodyn., 41 (2009) 790-798.
- [56] M.J.P. Comuñas, A. Baylaucq, C. Boned, J. Fernández, Int. J. thermophy., 22 (2001) 749-768.

- [57] J. Troncoso, D. Bessi eres, C.A. Cerdeiri a, E. Carballo, L. Roman  , J. Chem. Eng. Data, 49 (2004) 923-927.
- [58] J. Zhou, R. Zhu, H. Xu, Y. Tian, J. Chem. Eng. Data, 55 (2010) 5569-5575.
- [59] A. Gayol, L.M. Cas  s, R.E. Martini, A.E. Andreatta, J.L. Legido, J. Chem. Thermodyn., 58 (2013) 245-253.
- [60] W.V. Steele, R.D. Chirico, S.E. Knipmeyer, A. Nguyen J. Chem. Eng. Data, 42 (1997) 1008-1020.
- [61] F. Chen, Z. Yang, Z. Chen, J. Hu, C. Chen, J. Cai, J. Mol. Liq., 209 (2015) 683-692.
- [62] A. Rodriguez, J. Canosa, J. Tojo, J. Chem. Eng. Data, 46 (2001) 1476-1486.
- [63] J.M. Pardo, D. Gonz  lez-Salgado, C.A. Tovar, C.A. Cerdeiri a, E. Carballo, L. Roman  , Can. J. Chem., 80 (2002).370-378.
- [64] L. Mosteiro, A.B. Mariano, L.M. Cas  s, M.M. Pi  eiro, J.L. Legido, J. Chem. Eng. Data, 54 (2009) 1056-1062.
- [65] A. Pal, A. Kumar, J. Chem. Eng. Data, 43 (1998) 143-147.
- [66] M. Moosavi, A. Motahari, A. Vahid, V. Akbar, A.A. Rostami, A. Omrani, J. Chem. Eng. Data, 61 (2016) 1981-1991.
- [67] G.C. Benson, O. Kiyohara, J. Chem. Eng. Data 21 (1976) 362-365.
- [68] G. Douheret, M.I. Davis, J.C.R. Reis, M.J. Blandamer, Chem.Phys.Chem. 2 (2001) 148-161.
- [69] A.J. Costa, J. M. Esperanca I.M. Marrucho, L.P.N. Rebelo, J. Chem. Eng. Data 56 (2011) 3433-3441.
- [70] M.S. Reddy, Sk. Md Nayeem, C. Soumini, K.T.S.S. Raju, B.H. Babu, Thermochim. Acta. 630 (2016) 37-39.
- [71] S.M. Nayeem, M. Kondaiah, K. Sreekanth, M.S. Reddy, D.K. Rao, J. Therm. Anal. Calorim. 123 (2016) 2241-2255.
- [72] M.S. Reddy, K.T.S.S. Raju, A.S. Rao, N. Sharmila, B.H. Babu, J. Chem. Thermodyn. 101 (2016) 139-149.
- [73] P.K. Chhotaray, S. Jella, R.L. Gardas, J. Mol. Liq. 219 (2016) 829-844.
- [74] M.S. Reddy, Sk.Md. Nayeem, K.T.S.S. Raju, B.H. Babu, J. Therm. Anal. Calorim. 124 (2016) 959-971.

- [75] M. S. Reddy, K.T.S.S. Raju, Sk.Md. Nayeem, I. Khan, K.B.M. Krishna, B.H. Babu, J. Solution Chem. 45 (2016) 675-701.
- [76] A. Ali, F. Nabi, M. Tariq , Int. J. Thermophy. 30 (2009) 464-474.
- [77] E. Vercher, J.L. Francisco, A. Vicenta Gonzalez, J.M. Pablo, O. Vicent, M.A. Antoni, J. Chem. Thermodyn. 90 (2015) 174-184.
- [78] Z. Vaid, U.U. More, R.L. Gardas, N.L. Malek, S.P. Ijardar, J. Solution Chem. 44(2015) 718-741.
- [79] A. Ali, M. Tariq, J. Pure. App. Ultrason. 28 (2006) 99.
- [80] M.S. Reddy, Sk.Md. Nayeem, K.T.S.S. Raju, A.S. Rao, B.H. Babu, J. Mol. Liq. 218 (2016) 83-94.
- [81] C. Roth, A. Appelhagen, N. Jobst, R. Ludwig, Chem. Phys. Chem. 13 (2012) 1708-1717.
- [82] Sk.Md. Nayeem, I. Khan, Sk. Nyamathulla, D.S. Rao, P. Indira, M.S. Reddy, J. Mythri, P.N. Kumari. Proc of National seminar on 20-21 of Dec, 2016; ISBN: 978-93-85132-12-4.
- [83] B. Hartmann. J. Acoust. Soc. Am. 65 (1979) 1392-1396.
- [84] A.B. Copens, R.T. Beyer, J. Ballou. . J. Acoust. Soc. Am. 41 (1967) 1443-1448.
- [85] J. Jugan, M.A. Khadar. J Mol Liq. 100 (2002) 217-227.
- [86] Sk.Md. Nayeem, S. Nyamathulla, I. Khan, D.K. Rao. J Mol Liq. 218 (2016) 676-85.
- [87] P.A. Hunt, B. Kirchner, T. Welton, Chemi. A Europ. J. 12 (2006) 6762-6775.
- [88] A. Aggarwal, N.L. Lancaster, A.R. Sethi, T. Welton, Green Chem. 4 (2002) 517-520.
- [89] V. Znamenskiy, M.N. Kobrak, J. Phys. Chem. B. 108 (2004) 1072-1079.
- [90] N.R. Dhumal, H.J. Kim, J. Kiefer, J. Phys. Chem. A. 115 (2011) 3551-3558.
- [91] J. C. Lassegues, J. Grondin, D. Cavagnat, P. Johansson, New interpretation of the CH stretching vibrations in imidazolium-based ionic liquids, J. Phys. Chem. A. 113 (2009) 6419-6421.
- [92] J. C. Lassegues, J. Grondin, D. Cavagnat, P. Johansson, J. Phys. Chem. A. 114 (2009) 687-688.
- [93] J. Grondin, J. C. Lassegues, D. Cavagnat, T. Buffeteau, P. Johansson, R. Holomb, J. Raman Spectro. 42 (2011) 733-743.
- [94] N. Kristina, P. S. Schulz, P. Natalia, K. Johannes, P. Wasserscheid, A. Leipertz, Phys. Chem. Chem. Phys., 12(2010) 14153-14161

- [95] E. Vercher, F. J. Llopis, M. V. Gonzalez-Alfaro, A. M. Andreu, J. Chem. Eng. Data 55(2010) 1377-1388 .
- [96] D. Patterson, G. Delmas, Discuss. Faraday Soc. 49(1970) 98-105.
- [97] M. T. Zafarani-Moattar, H. Shekaari, J. Chem. Thermodyn. 38(2006) 1377-1384.
- [98] F. Kermanpour, H. Z. Niakan, J. Chem. Thermodyn. 48(2012) 129-139 .
- [99] R.B. Torres, M.I. Ortolan, P.L.O. Volpe, J. Chem. Thermodyn. 40 (2008) 442-459.
- [100] P. J. Flory, J. Am. Chem. Soc. 87(1965) 1833-1838 .
- [101] A. Abe, P. J. Flory, J. Am. Chem. Soc. 87 (1965) 1838-1846.
- [102] E. Vercher, A. V. Orchilles, P. J. Miguel, A. M. Andreu, J. Chem. Eng. Data 52(2007) 1468-1482.
- [103] A. Kumar, T. Singh, R. L. Gardas, J.A. Coutinho, J. Chem. Thermodyn. 40 (2008) 32-39.
- [104] Z. S. Vaid, U. U More, S. B. Oswal, N.I. Malek, Thermochim. Acta, 634 (2016) 38-47.

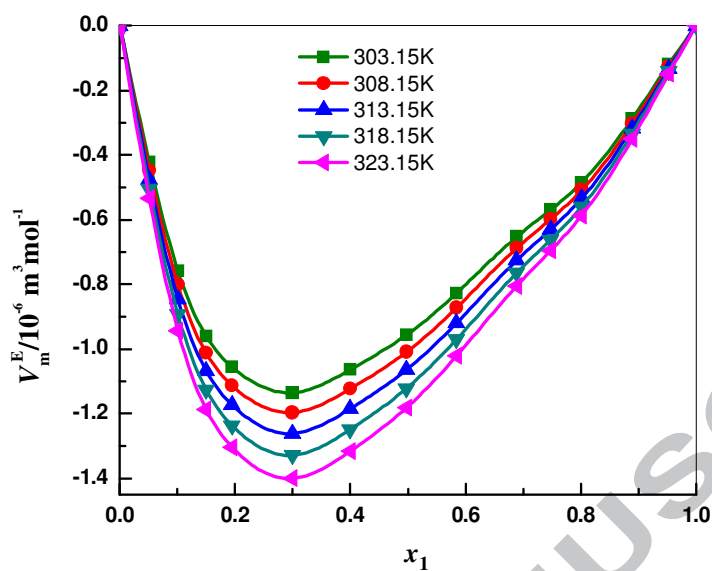


Fig. 1 Plots of excess molar volume (V_m^E) against mole fraction of [Bmim][NTF₂] in the mixture with DMC at different temperatures.

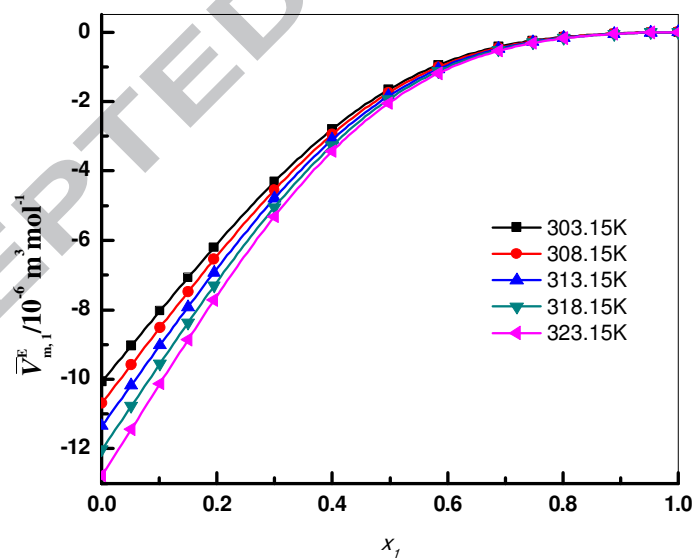


Fig.2 Plots of excess partial molar volume ($\bar{V}_{m,1}^E$) against mole fraction of [Bmim][NTF₂] in the mixture with DMC at different temperatures.

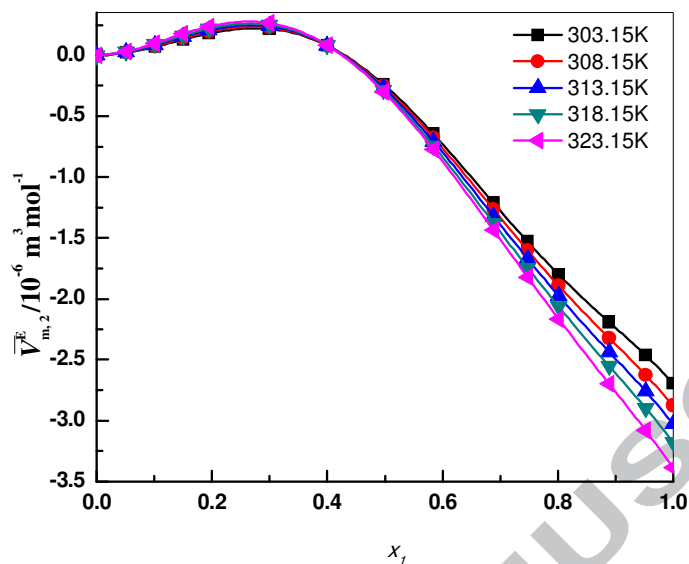


Fig. 3 Plots of excess partial molar volume ($\bar{V}_{m,2}^E$) against mole fraction of [Bmim][NTF₂] in the mixture with DMC at different temperatures.

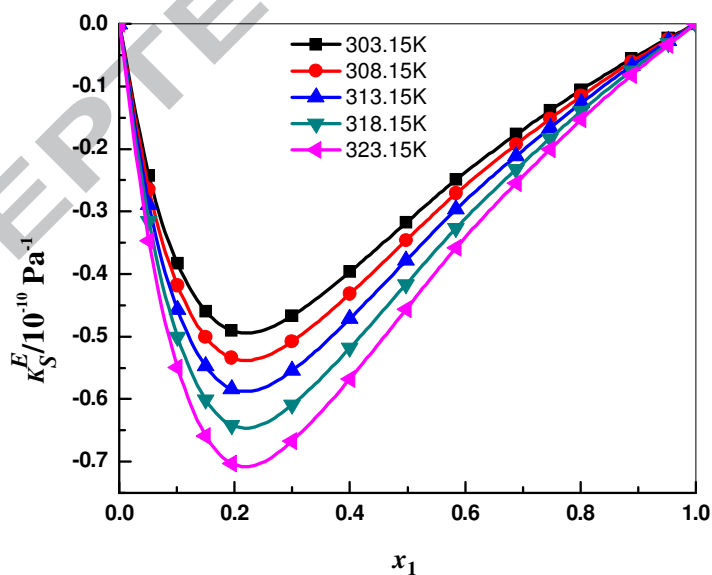


Fig. 4 Plots of excess isentropic compressibility (κ_S^E) against mole fraction of [Bmim][NTF₂] in the mixture with DMC at different temperatures.

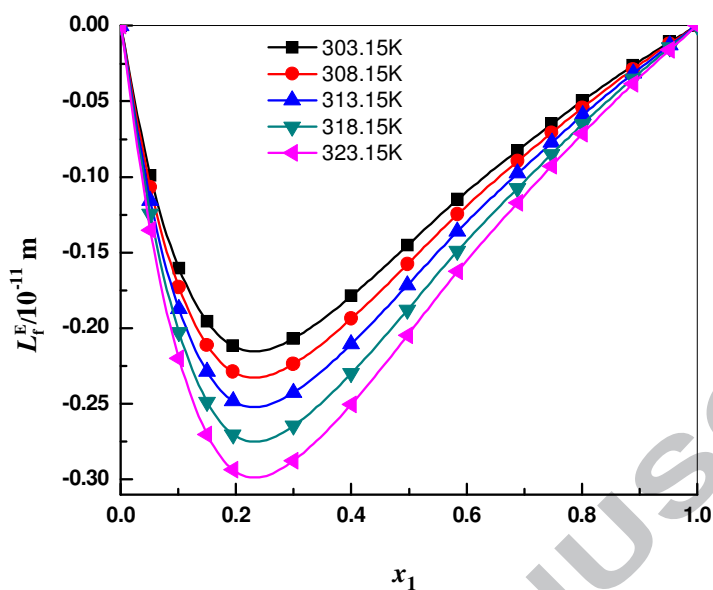


Fig. 5 Plots of excess free length (L_f^E) against mole fraction of [Bmim][NTF₂] in the mixture with DMC at different temperatures.

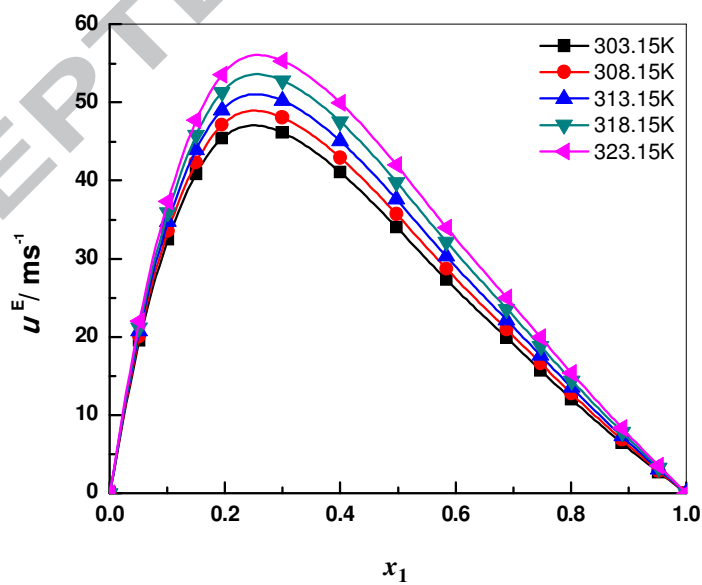


Fig.6 Plots of Excess ultrasonic speed of sounds (u^E) against mole fraction of [Bmim][NTF₂] in the mixture with DMC at different temperatures.

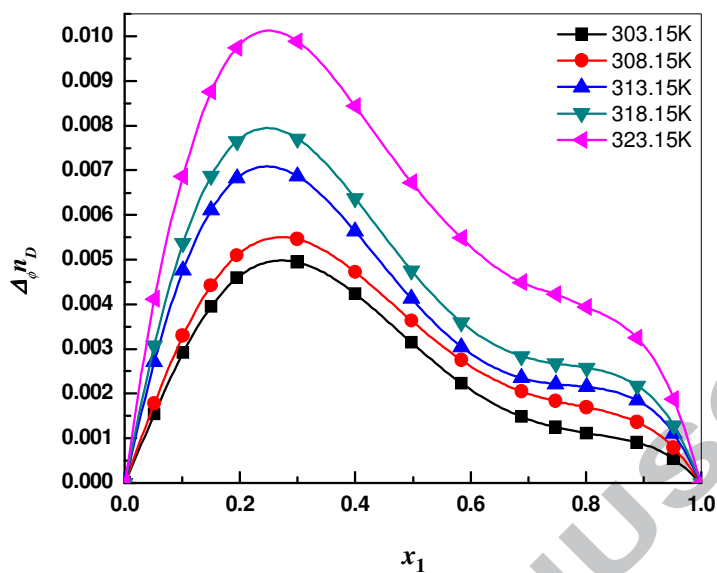


Fig. 7 Plots of deviation in refractive index (Δn_D) against mole fraction of [Bmim][NTF₂] in the mixture with DMC at different temperatures.

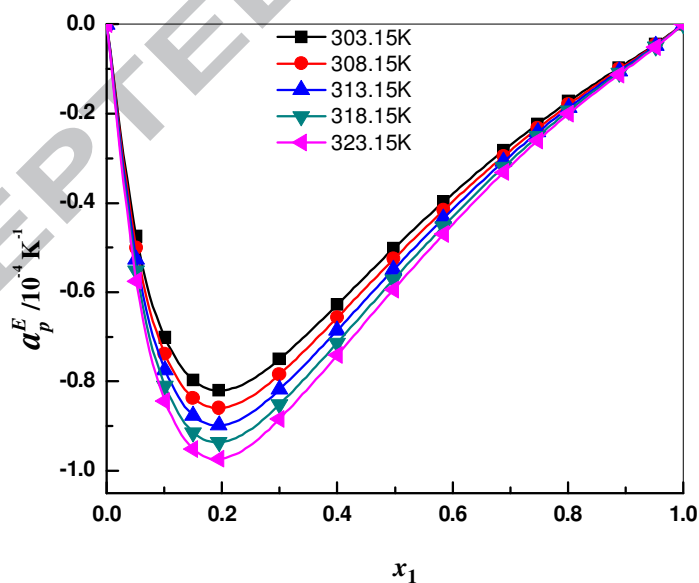


Fig. 8 Plots of Excess isobaric thermal expansion coefficient (α_p^E) against mole fraction of [Bmim][NTF₂] in the mixture with DMC at different temperatures.

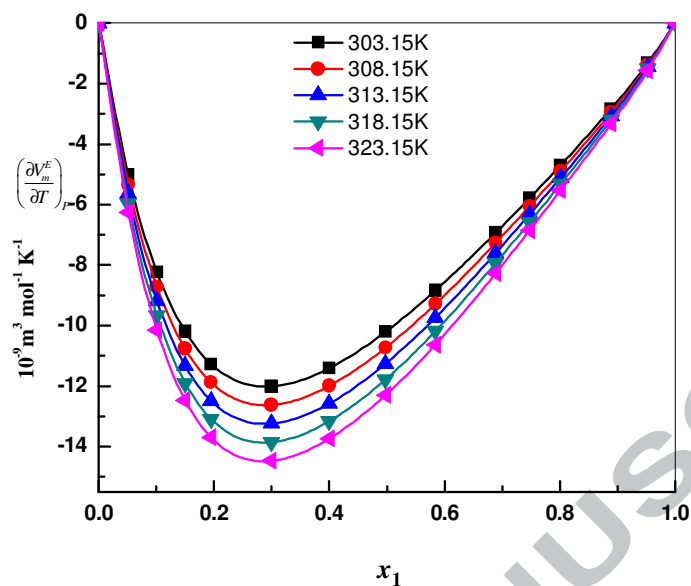


Fig. 9 Plots of $\left(\frac{\partial V_m^E}{\partial T}\right)_P$ against mole fraction of [Bmim][NTF₂] in the mixture with DMC at different temperatures.

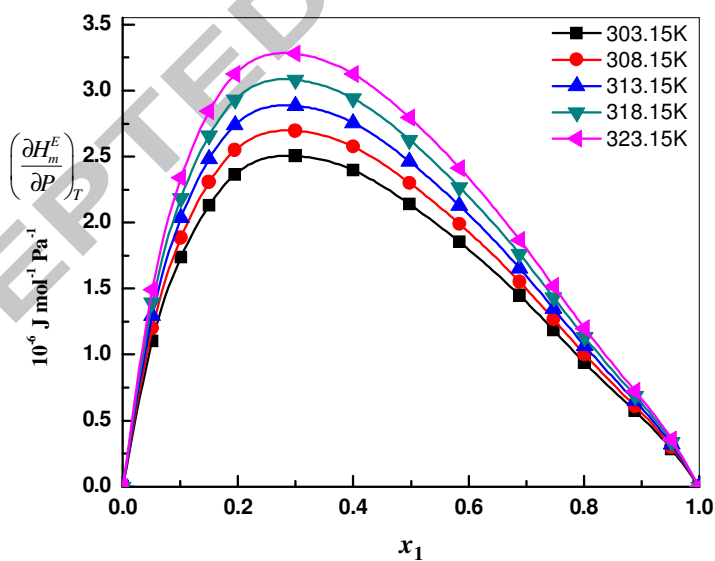


Fig. 10 Plots of $\left(\frac{\partial H_m^E}{\partial P}\right)_T$ against mole fraction of [Bmim][NTF₂] in the mixture with DMC at different temperatures.

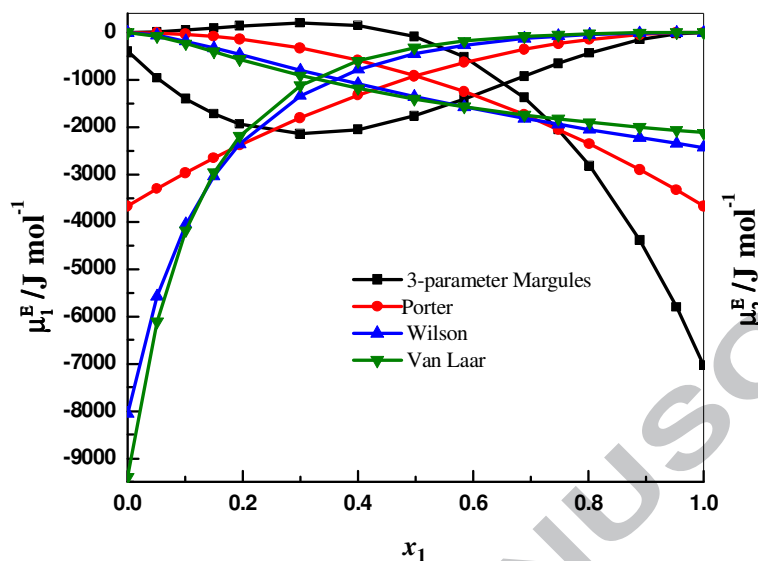


Fig.11 Variation of excess chemical potentials μ_1^E ([Bmim][NTf₂]) and μ_2^E (DMC) with mole fraction, x_1 of [Bmim][NTf₂] for 3-parameter Margules, Porter, Wilson and Van Laar at T=308.15 K.

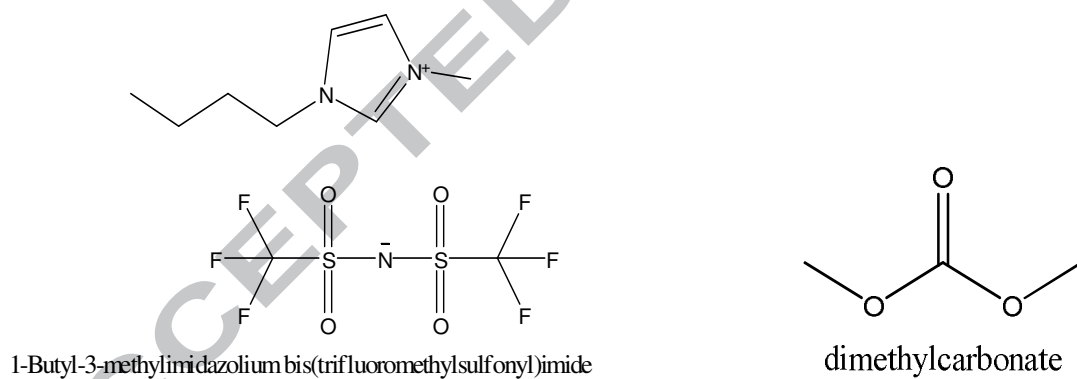


Fig.12 Chemical Structures of ([Bmim][NTf₂]) and DMC.

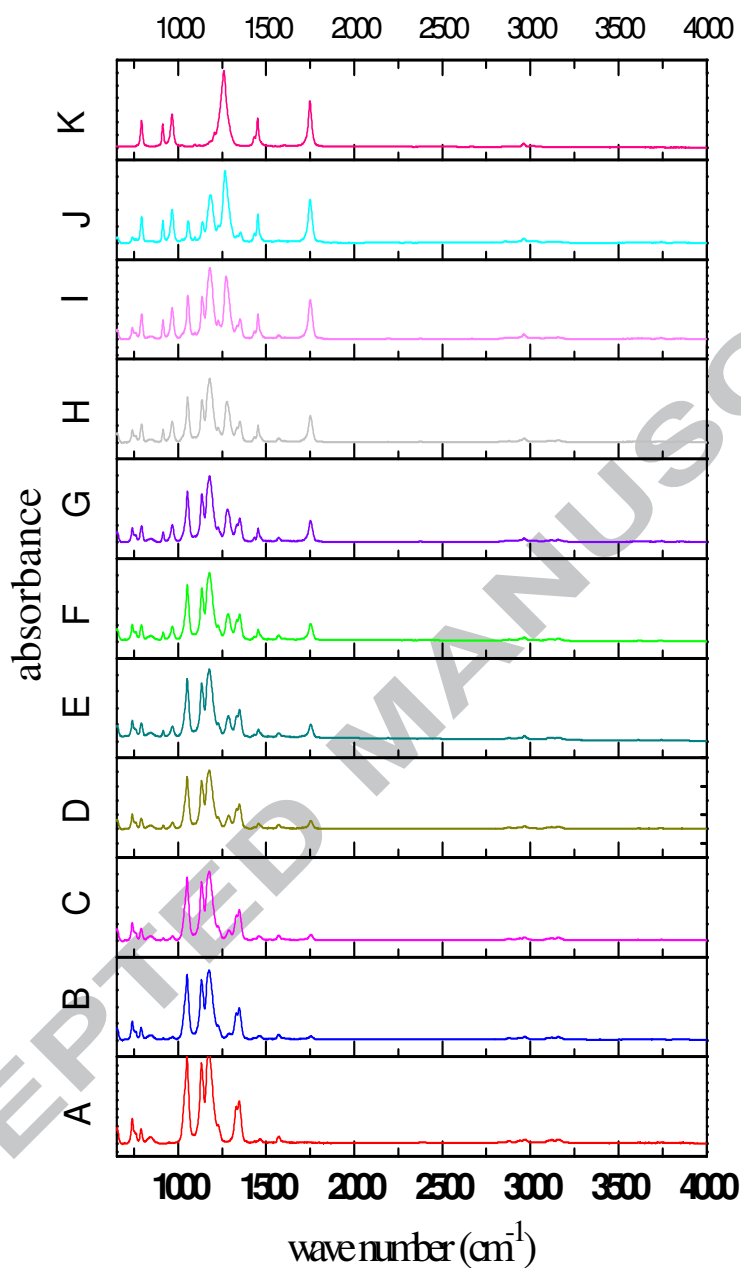


Fig.13 Infrared spectra of (A) Pure IL [Bmim][NTf₂]; (B) 0.8990; (C) 0.8055; (D) 0.7006; (E) 0.6001; (F) 0.5024; (G) 0.4158; (H) 0.3114; (I) 0.2525; (J) 0.1110 and (K) Pure DMC. (B), (C), (D), (E), (F), (G), (H), (I), (J) represents mole fraction of [Bmim][NTf₂] in the mixture with DMC.

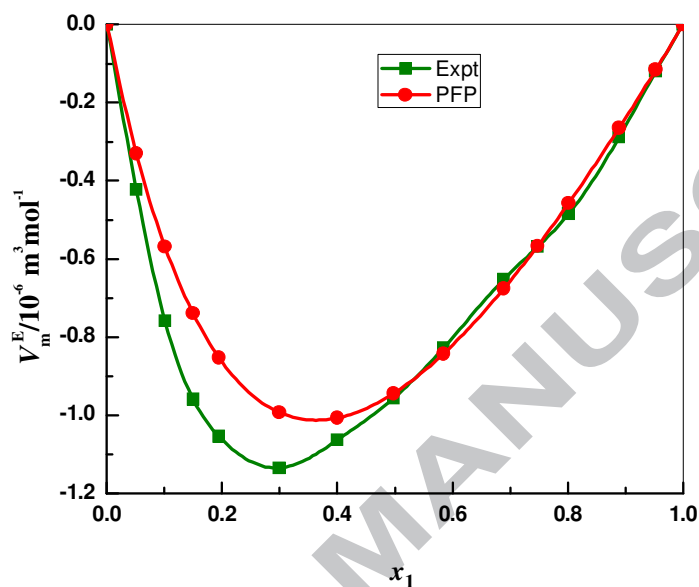


Fig. 14 Plots of excess molar volumes (V_m^E) of experimental and calculated from PFP theory against mole fraction of [Bmim][NTf₂] in the mixture with DMC at 303.15K.

Table 1 List of chemicals with details of Provenance, CAS number, and mass fraction purity.

Chemical name (CAS number)	Provenance	Purification method	Mass fraction purity	Analysis method	Final water mass fraction	Water Analysis method
1-butyl-3-methylimidazoliumbis (trifluoromethylsulfonyl)imide (174899-83-3)	Io-Li-Tec, Germany	Vacuum treatment	0.99 [*]	NA	$<1.5 \times 10^{-4}$	K.F
Dimethyl carbonate (616-38-6)	Sigma Aldrich	Distillation	0.995	GC	$<1.5 \times 10^{-4}$	K.F

*Purity as given by the suppliers, K.F= Karl Fisher Titrator, GC= Gas Chromatography.

Table 2 Comparison of experimental values of density, ρ , speed of sound, u , refractive index, n_D , and specific heat, C_p , of pure liquids with the corresponding literature values at different temperatures and at atmospheric pressure $P = 101.3$ kPa.

Liquid	$T /$ K	$\rho / \text{kg} \cdot \text{m}^{-3}$		$u / \text{m} \cdot \text{s}^{-1}$		n_D		$C_p / \text{J} \cdot \text{K}^{-1} \cdot \text{mol}^{-1}$
		Expt.	Lit.	Expt.	Lit.	Expt.	Lit.	
[Bmim][NTF ₂]	303.15	1428.9	1429.40[32] 1429.31[44] 1430.81[54]	1216.8	1216.77[38] 1217.5[53]	1.4245	1.42523[38] 1.4250[54]	569.74[44]
	308.15	1424.1	1424.57[32] 1424.54[44]	1205.8	1205.80[38] 1205.23[53]	1.4231	1.42374[38]	572.82[44]
	313.15	1419.4	1419.61[32] 1419.78[44] 1420.16[54]	1195.0	1194.95[38] 1194.36[53]	1.4210	1.42225[38] 1.4214[54]	575.56[44]
	318.15	1414.6	1414.67[32] 1415.04[44]	1184.2	1184.23[38] 1184.54[53]	1.4195	1.42076[38]	578.49[44]
	323.15	1409.9	1409.65[32] 1410.31[44] 1411.55[54]	1173.6	1173.61[38] 1171.35[53]	1.4173	1.41923[38] 1.4185[54]	581.68[44]
Dimethyl carbonate	303.15	1056.8	1056.719[41] 1056.632[61]	1177.3	1177[42] 1177[62] 1173.5[64]	1.3648	1.3640[43] 1.36414[62]	159.8[45]
	308.15	1050.2	1050.071[41] 1049.983[61]	1155.6	1155[42] 1151.5[64]	1.3629	1.3618[43] 1.3661[64]	161.7[45]
	313.15	1043.5	1043.388[41] 1043.307[61]	1134.2	1134[42] 1135[62]	1.3626	1.3595[43] 1.35932[62]	162.9[45]
	318.15	1036.8	1036.687[41] 1036.59[61]	1113.1	-	1.3601	1.3570[43] 1.3629[64]	163.0[45]
	323.15	1030.0	1029.939[41] 1029.843[61]	1092.2	-	1.3586	-	163.6[45]

Standard uncertainties u are: $u(\rho) = 1 \text{ kg} \cdot \text{m}^{-3}$, $u(u) = 0.5 \text{ m} \cdot \text{s}^{-1}$, $u(n_D) = 0.0005$, $u(T) = 0.01 \text{ K}$ and $u(P) = 0.5 \text{ kPa}$

Table 3 Experimental density (ρ), speed of sound (u), refractive index (n_D), molar volume (V_m), Isentropic compressibility (κ_s), free length (L_f) and isobaric thermal expansion coefficient (α_p) with mole fraction (x_1) of [Bmim][NTF₂] in the binary liquid mixture of {[Bmim][NTF₂]+Dimethyl Carbonate} from $T/K = 303.15$ to 323.15 at pressure $P = 101.3$ kPa.

x_1	$\rho /$ $\text{kg}\cdot\text{m}^{-3}$	$u /$ $\text{m}\cdot\text{s}^{-1}$	n_D	$V_m /$ $10^{-6} \text{ m}^3\cdot\text{mol}^{-1}$	$\kappa_s /$ 10^{-10} Pa^{-1}	L_f $/10^{-11} \text{ m}$	α_p $/10^{-4} \text{ K}^{-1}$
303.15 K							
0.0000	1056.8	1177.3	1.3648	85.24	6.83	5.423	12.54
0.0512	1120.1	1187.0	1.3757	95.48	6.34	5.225	11.15
0.1010	1168.9	1196.1	1.3844	105.51	5.98	5.076	10.21
0.1495	1207.1	1203.7	1.3913	115.41	5.72	4.963	9.54
0.1945	1236.1	1209.2	1.3965	124.69	5.53	4.882	9.07
0.2994	1288.3	1215.4	1.4053	146.45	5.25	4.758	8.32
0.3999	1324.3	1217.4	1.4106	167.44	5.09	4.685	7.85
0.4976	1351.4	1217.7	1.4141	187.90	4.99	4.637	7.53
0.5842	1370.7	1217.4	1.4165	206.06	4.92	4.605	7.31
0.6886	1389.7	1217.4	1.4191	227.99	4.86	4.573	7.11
0.7475	1399.0	1217.2	1.4204	240.33	4.82	4.559	7.01
0.8014	1406.6	1217.0	1.4216	251.65	4.80	4.547	6.93
0.8890	1417.4	1216.8	1.4233	270.09	4.76	4.531	6.82
0.9526	1424.2	1216.8	1.4242	283.49	4.74	4.520	6.75
1.0000	1428.9	1216.8	1.4245	293.48	4.73	4.513	6.71
308.15 K							
0.0000	1050.2	1155.6	1.3629	85.78	7.13	5.592	12.68
0.0512	1113.8	1167.2	1.3741	96.01	6.59	5.377	11.25
0.1010	1163.0	1177.7	1.3830	106.05	6.20	5.215	10.28
0.1495	1201.3	1186.5	1.3900	115.96	5.91	5.093	9.60
0.1945	1230.5	1192.9	1.3953	125.26	5.71	5.005	9.12
0.2994	1282.9	1200.7	1.4042	147.06	5.41	4.870	8.35
0.3999	1319.1	1203.8	1.4095	168.10	5.23	4.790	7.87
0.4976	1346.3	1204.9	1.4131	188.61	5.12	4.737	7.54

0.5842	1365.6	1205.0	1.4155	206.82	5.04	4.703	7.32
0.6886	1384.8	1205.5	1.4181	228.80	4.97	4.669	7.11
0.7475	1394.1	1205.6	1.4195	241.17	4.94	4.653	7.01
0.8014	1401.8	1205.6	1.4207	252.52	4.91	4.640	6.93
0.8890	1412.6	1205.6	1.4223	271.01	4.87	4.622	6.82
0.9526	1419.4	1205.7	1.4230	284.45	4.85	4.610	6.75
1.0000	1424.1	1205.8	1.4231	294.47	4.83	4.602	6.71

313.15 K

0.0000	1043.5	1134.2	1.3626	86.33	7.45	5.767	12.83
0.0512	1107.5	1147.5	1.3744	96.56	6.86	5.533	11.35
0.1010	1157.0	1159.4	1.3836	106.60	6.43	5.358	10.36
0.1495	1195.5	1169.4	1.3907	116.52	6.12	5.226	9.65
0.1945	1224.9	1176.8	1.3959	125.83	5.90	5.131	9.16
0.2994	1277.6	1186.2	1.4042	147.68	5.56	4.984	8.37
0.3999	1313.9	1190.3	1.4089	168.77	5.37	4.897	7.89
0.4976	1341.2	1192.1	1.4119	189.32	5.25	4.840	7.55
0.5842	1360.7	1192.8	1.4140	207.58	5.17	4.803	7.33
0.6886	1379.8	1193.7	1.4166	229.62	5.09	4.765	7.11
0.7475	1389.2	1194.0	1.4180	242.02	5.05	4.748	7.01
0.8014	1396.9	1194.2	1.4193	253.40	5.02	4.734	6.93
0.8890	1407.8	1194.5	1.4208	271.93	4.98	4.715	6.82
0.9526	1414.6	1194.8	1.4213	285.41	4.95	4.702	6.75
1.0000	1419.4	1195.0	1.4210	295.46	4.93	4.694	6.71

318.15 K

0.0000	1036.8	1113.1	1.3601	86.88	7.78	5.948	12.98
0.0512	1101.2	1127.6	1.3724	97.11	7.14	5.697	11.45
0.1010	1151.0	1141.0	1.3819	107.15	6.67	5.507	10.43
0.1495	1189.8	1152.4	1.3892	117.09	6.33	5.363	9.71
0.1945	1219.3	1160.8	1.3946	126.41	6.09	5.260	9.21
0.2994	1272.2	1171.7	1.4030	148.30	5.73	5.101	8.40
0.3999	1308.8	1176.9	1.4077	169.43	5.52	5.007	7.91

0.4976	1336.2	1179.5	1.4107	190.04	5.38	4.945	7.56
0.5842	1355.7	1180.6	1.4128	208.34	5.29	4.904	7.33
0.6886	1374.9	1182.1	1.4154	230.43	5.20	4.864	7.12
0.7475	1384.3	1182.6	1.4168	242.87	5.16	4.845	7.02
0.8014	1392.1	1183.0	1.4181	254.28	5.13	4.830	6.93
0.8890	1403.0	1183.6	1.4196	272.86	5.09	4.809	6.81
0.9526	1409.9	1184.0	1.4199	286.38	5.06	4.795	6.74
1.0000	1414.6	1184.2	1.4195	296.45	5.04	4.786	6.70
323.15 K							
0.0000	1030.0	1092.2	1.3586	87.45	8.14	6.135	13.13
0.0512	1094.9	1108.3	1.3719	97.67	7.44	5.864	11.56
0.1010	1145.0	1123.0	1.3817	107.72	6.92	5.659	10.51
0.1495	1184.0	1135.6	1.3893	117.66	6.55	5.504	9.77
0.1945	1213.7	1144.9	1.3948	127.00	6.29	5.392	9.26
0.2994	1266.9	1157.4	1.4033	148.92	5.89	5.220	8.44
0.3999	1303.6	1163.6	1.4078	170.11	5.67	5.119	7.93
0.4976	1331.1	1166.9	1.4106	190.76	5.52	5.051	7.58
0.5842	1350.7	1168.6	1.4126	209.10	5.42	5.008	7.34
0.6886	1370.1	1170.5	1.4149	231.26	5.33	4.964	7.12
0.7475	1379.5	1171.3	1.4162	243.73	5.28	4.943	7.02
0.8014	1387.3	1171.8	1.4172	255.16	5.25	4.927	6.93
0.8890	1398.2	1172.7	1.4185	273.79	5.20	4.904	6.81
0.9526	1405.1	1173.3	1.4183	287.34	5.17	4.890	6.74
1.0000	1409.9	1173.6	1.4173	297.44	5.15	4.880	6.70

Standard uncertainties u are: $u(x_1) = 0.0005$, $u(\rho) = 1 \text{ kg}\cdot\text{m}^{-3}$, $u(u) = 0.5 \text{ m}\cdot\text{s}^{-1}$, $u(n_D) = 0.0005$, $u(T) = 0.01 \text{ K}$ and $u(P) = 0.5 \text{ kPa}$

Combined uncertainties (Confidence level, 95%): $U_c(V_m) = \pm 0.01 \times 10^{-6} \text{ m}^3\cdot\text{mol}^{-1}$, $U_c(\kappa_s) = \pm 0.01 \times 10^{-10} \text{ Pa}^{-1}$, $U_c(L_f) = \pm 0.004 \times 10^{-11}$

m , $U_c(\alpha_p) = \pm 0.02 \times 10^{-4} \text{ K}^{-1}$. All the experiments were carried out at atmospheric pressure.

Table 4 Redlich-Kister coefficients of deviation/excess properties and corresponding standard deviations (σ) for the systems at different temperatures

	T/K	A_0	A_1	A_2	A_3	A_4	σ
$V_m^E / 10^{-6} \text{ m}^3 \cdot \text{mol}^{-1}$	303.15	-3.7691	2.7718	-3.1693	0.9125	0.5598	0.0116
	308.15	-3.9776	2.9260	-3.2755	0.9779	0.4746	0.0116
	313.15	-4.1973	3.0796	-3.3947	1.0777	0.4088	0.0116
	318.15	-4.4264	3.2397	-3.5207	1.1823	0.3486	0.0118
	323.15	-4.6667	3.4168	-3.6344	1.2738	0.2268	0.0118
$\kappa_s^E / 10^{-10} \text{ Pa}^{-1}$	303.15	-1.2590	1.6018	-1.5522	1.1085	-0.3642	0.0009
	308.15	-1.3716	1.7399	-1.6863	1.2149	-0.4139	0.0010
	313.15	-1.4992	1.8959	-1.8365	1.3357	-0.4696	0.0011
	318.15	-1.6475	2.0902	-2.0444	1.4293	-0.4468	0.0016
	323.15	-1.8056	2.2819	-2.2271	1.5892	-0.5319	0.0017
$u^E / \text{ m} \cdot \text{s}^{-1}$	303.15	134.83	-155.38	131.88	-47.51	-17.82	0.19
	308.15	141.47	-161.03	135.73	-46.27	-20.48	0.20
	313.15	148.90	-167.28	139.80	-44.99	-23.30	0.21
	318.15	157.59	-175.62	147.18	-40.03	-33.20	0.27
	323.15	166.23	-182.49	151.30	-39.45	-34.95	0.29
$I_f^E / (10^{-11} \text{ m})$	303.15	-0.5757	0.7055	-0.6564	0.3768	-0.0557	0.0005
	308.15	-0.6244	0.7609	-0.7064	0.4041	-0.0616	0.0006
	313.15	-0.6793	0.8228	-0.7615	0.4346	-0.0678	0.0007
	318.15	-0.7429	0.8996	-0.8382	0.4507	-0.0399	0.0010
	323.15	-0.8100	0.9741	-0.9033	0.4909	-0.0533	0.0010
$\alpha_p^E 10^{-4} \text{ K}^{-1}$	303.15	-2.0062	2.3457	-2.2104	2.9501	-2.3566	0.0058
	308.15	-2.0998	2.4468	-2.2782	3.1473	-2.5624	0.0062
	313.15	-2.1919	2.5464	-2.3451	3.3387	-2.7621	0.0066

	318.15	-2.2829	2.6448	-2.4102	3.5244	-2.9575	0.0070
	323.15	-2.3725	2.7411	-2.4742	3.7052	-3.1455	0.0074
	303.15	0.01245	-0.02333	0.01845	0.01435	-0.00846	0.00002
	308.15	0.01069	-0.01352	0.03020	-0.02158	-0.00363	0.00059
	313.15	0.01634	-0.02940	0.03592	0.01380	-0.00810	0.00002
$\Delta \phi^{n_D}$	318.15	0.01884	-0.03157	0.04000	0.01390	-0.00815	0.00002
	323.15	0.02677	-0.03442	0.04592	0.01220	-0.00213	0.00005
	303.15	-40.7100	29.0818	-22.2609	15.2811	-11.9823	0.00002
$\left(\frac{\partial V_m^E}{\partial T}\right)_P$	308.15	-42.7938	30.5777	-22.8838	16.9091	-13.9121	0.00002
$/10^{-9} \text{m}^3 \cdot \text{mol}^{-1} \cdot \text{K}^{-1}$	313.15	-44.8774	32.0734	-23.5063	18.5380	-15.8427	0.00001
	318.15	-46.9612	33.5688	-24.1286	20.1673	-17.7740	0.00001
	323.15	-49.0449	35.0647	-24.7526	21.7959	-19.7029	0.00002
	303.15	8.5721	-6.0444	3.5792	-3.7197	4.1920	0.0116
$\left(\frac{\partial H_m^E}{\partial P}\right)_T$	308.15	9.2093	-6.4965	3.7762	-4.2328	4.7616	0.0116
$/10^{-6} \text{J} \cdot \text{mol}^{-1} \cdot \text{Pa}^{-1}$	313.15	9.8560	-6.9642	3.9665	-4.7275	5.3698	0.0116
	318.15	10.5142	-7.4404	4.1562	-5.2338	6.0028	0.0118
	323.15	11.1822	-7.9144	4.3643	-5.7694	6.5939	0.0118

Table 5 Partial molar volumes of component-1 ($\bar{V}_{m,1}$) ([Bmim][NTF₂]) and component-2 ($\bar{V}_{m,2}$) (Dimethyl Carbonate) with mole fraction (x_1) of [Bmim][NTF₂] in the binary liquid mixture from $T/K=303.15$ to 323.15 at pressure $P = 101.3$ kPa.

x_1	303.15 K		308.15 K		313.15 K		318.15 K		323.15 K	
	$\bar{V}_{m,1}$	$\bar{V}_{m,2}$	$\bar{V}_{m,1}$	$\bar{V}_{m,2}$	$\bar{V}_{m,1}$	$\bar{V}_{m,2}$	$\bar{V}_{m,1}$	$\bar{V}_{m,2}$	$\bar{V}_{m,1}$	$\bar{V}_{m,2}$
	/ $10^{-6} \text{ m}^3 \cdot \text{mol}^{-1}$		/ $10^{-6} \text{ m}^3 \cdot \text{mol}^{-1}$		/ $10^{-6} \text{ m}^3 \cdot \text{mol}^{-1}$		/ $10^{-6} \text{ m}^3 \cdot \text{mol}^{-1}$		/ $10^{-6} \text{ m}^3 \cdot \text{mol}^{-1}$	
0.0000	283.42	85.24	283.79	85.78	284.12	86.33	284.43	86.88	284.68	87.45
0.0512	284.45	85.26	284.88	85.80	285.29	86.35	285.68	86.91	286.01	87.48
0.1010	285.45	85.31	285.95	85.85	286.43	86.41	286.90	86.98	287.32	87.55
0.1495	286.41	85.37	286.99	85.92	287.54	86.48	288.08	87.05	288.59	87.63
0.1945	287.28	85.42	287.92	85.97	288.53	86.53	289.14	87.10	289.72	87.69
0.2994	289.16	85.45	289.92	86.00	290.67	86.56	291.40	87.14	292.13	87.72
0.3999	290.69	85.32	291.52	85.86	292.36	86.41	293.19	86.97	294.01	87.54
0.4976	291.82	85.00	292.72	85.52	293.61	86.06	294.51	86.60	295.39	87.15
0.5842	292.53	84.59	293.46	85.10	294.39	85.62	295.33	86.14	296.25	86.68
0.6886	293.06	84.02	294.02	84.51	294.98	85.00	295.94	85.50	296.90	86.01
0.7475	293.23	83.71	294.20	84.17	295.18	84.65	296.15	85.14	297.13	85.63
0.8014	293.34	83.44	294.32	83.88	295.29	84.35	296.28	84.82	297.26	85.29
0.8890	293.43	83.04	294.42	83.45	295.41	83.89	296.40	84.33	297.39	84.75
0.9526	293.47	82.77	294.46	83.15	295.45	83.56	296.44	83.99	297.43	84.37
1.0000	293.48	82.54	294.47	82.90	295.46	83.30	296.45	83.71	297.44	84.07

Standard uncertainties u are $u(x_1) = 0.0005$, $u(\rho) = 1 \text{ kg m}^{-3}$, $u(T) = 0.01 \text{ K}$ and $u(P) = 0.5 \text{ kPa}$

Combined uncertainties (Confidence level, 95%): $U(\bar{V}_{m,1}) = \pm 0.02 \times 10^{-6} \text{ m}^3 \cdot \text{mol}^{-1}$, $U(\bar{V}_{m,2}) = \pm 0.02 \times 10^{-6} \text{ m}^3 \cdot \text{mol}^{-1}$

Table 6 Partial molar volumes at infinite dilution ($\bar{V}_{m,1}^{\infty}, \bar{V}_{m,2}^{\infty}$) and excess partial molar volumes at infinite dilution ($\bar{V}_{m,1}^{E,\infty}, \bar{V}_{m,2}^{E,\infty}$) of [Bmim][NTF₂] and Dimethyl Carbonate at $T = (303.15, 308.15, 313.15, 318.15 \text{ and } 323.15) \text{ K}$.

T/K	$\bar{V}_{m,1}^{\infty}$	$\bar{V}_{m,1}^{E,\infty}$	$\bar{V}_{m,2}^{\infty}$	$\bar{V}_{m,2}^{E,\infty}$
	$/10^{-6} \text{ m}^3 \cdot \text{mol}^{-1}$		$/10^{-6} \text{ m}^3 \cdot \text{mol}^{-1}$	
303.15	283.42	-10.06	82.55	-2.69
308.15	283.79	-10.68	82.91	-2.87
313.15	284.12	-11.34	83.30	-3.03
318.15	284.43	-12.02	83.70	-3.18
323.15	284.68	-12.76	84.07	-3.38

Combined uncertainties (Confidence level, 95%): $U(\bar{V}_{m,1}^{E,\infty}) = \pm 0.02 \times 10^{-6} \text{ m}^3 \cdot \text{mol}^{-1}$, $U(\bar{V}_{m,2}^{E,\infty}) = \pm 0.02 \times 10^{-6} \text{ m}^3 \cdot \text{mol}^{-1}$

Table 7

Computed excess values of $(B/A)^E$, cohesive energy (ΔA), Van der Waal's constants (a & b), distance of closest approach (d), from non-linear parameters proposed by Hartmann–Balizar ($B\&H$) and Ballou relations

$(B/A)^E$	ΔA	a	b	d	$(B/A)^E$	ΔA	a	b	d
	$/J \cdot mol^{-1}$	$/N \cdot m^4 \cdot mol^{-1}$	$/10^{-3} m^3 \cdot mol^{-1}$	$/10^{-10} m$		$/ J \cdot mol^{-1}$	$/N \cdot m^4 \cdot mol^{-1}$	$/10^{-3} m^3 \cdot mol^{-1}$	$/10^{-10} m$
Hartmann-Balazar					Ballou				
T=303.15 K									
0.0000	-188292.0015	0.9338	0.0656	3.7338	0.0000	-199408.6326	0.9890	0.0667	3.7544
-0.0545	-229412.5970	1.2710	0.0774	3.9448	-0.0667	-243395.2996	1.3485	0.0784	3.9624
-0.1033	-270796.2088	1.6545	0.0886	4.1259	-0.1265	-287780.0498	1.7583	0.0896	4.1413
-0.1423	-311827.4368	2.0808	0.0993	4.2861	-0.1742	-331851.9850	2.2144	0.1002	4.3001
-0.1670	-349807.5325	2.5190	0.1091	4.4235	-0.2045	-372646.3641	2.6835	0.1101	4.4364
-0.1801	-435268.5564	3.6739	0.1317	4.7100	-0.2206	-464216.9518	3.9183	0.1327	4.7209
-0.1664	-514746.7969	4.9608	0.1532	4.9530	-0.2037	-549184.4722	5.2927	0.1541	4.9626
-0.1420	-590547.5032	6.3802	0.1740	5.1673	-0.1739	-630092.2220	6.8074	0.1748	5.1759
-0.1167	-656969.1007	7.7782	0.1923	5.3429	-0.1429	-700924.3264	8.2987	0.1932	5.3509
-0.0883	-737512.2039	9.6542	0.2144	5.5404	-0.1082	-786851.9245	10.3001	0.2153	5.5477
-0.0713	-782634.4973	10.7958	0.2268	5.6454	-0.0873	-834966.8813	11.5177	0.2277	5.6524
-0.0553	-823857.5219	11.8964	0.2382	5.7383	-0.0678	-878912.5186	12.6914	0.2391	5.7450
-0.0304	-890984.1988	13.8031	0.2568	5.8834	-0.0372	-950490.1335	14.7250	0.2576	5.8898
-0.0129	-939846.3372	15.2789	0.2702	5.9845	-0.0158	-1002606.4218	16.2992	0.2711	5.9906
0.0000	-976342.1751	16.4287	0.2803	6.0577	0.0000	-1041537.4309	17.5258	0.2811	6.0636
T=308.15 K									
0.0000	-179133.0308	0.8988	0.0648	3.7181	0.0000	-188946.8254	0.9481	0.0659	3.7388
-0.0657	-219270.2249	1.2273	0.0768	3.9341	-0.0805	-231779.7091	1.2973	0.0778	3.9518
-0.1230	-259813.0869	1.6022	0.0881	4.1183	-0.1506	-275171.1391	1.6970	0.0891	4.1339
-0.1680	-300095.5321	2.0198	0.0989	4.2808	-0.2057	-318355.7598	2.1427	0.0999	4.2949
-0.1965	-337437.0551	2.4498	0.1089	4.4197	-0.2406	-358394.1605	2.6020	0.1098	4.4327
-0.2129	-421473.6884	3.5839	0.1316	4.7084	-0.2607	-448294.1925	3.8119	0.1325	4.7194

-0.1983	-499662.4223	4.8488	0.1532	4.9527	-0.2428	-531759.8887	5.1603	0.1541	4.9624
-0.1709	-574208.5057	6.2447	0.1740	5.1679	-0.2093	-611212.7531	6.6471	0.1749	5.1766
-0.1416	-639467.9287	7.6195	0.1924	5.3441	-0.1734	-680700.2884	8.1108	0.1933	5.3522
-0.1080	-718694.2379	9.4661	0.2146	5.5422	-0.1322	-765102.5937	10.0774	0.2155	5.5496
-0.0877	-763076.5675	10.5901	0.2271	5.6475	-0.1074	-812361.2896	11.2741	0.2280	5.6546
-0.0684	-803592.8396	11.6735	0.2385	5.7407	-0.0838	-855489.6602	12.4274	0.2394	5.7475
-0.0379	-869575.9858	13.5508	0.2571	5.8861	-0.0465	-925744.2793	14.4260	0.2580	5.8926
-0.0162	-917574.4702	15.0037	0.2706	5.9875	-0.0198	-976861.0838	15.9731	0.2715	5.9936
0.0000	-953399.3579	16.1355	0.2807	6.0608	0.0000	-1015015.6349	17.1783	0.2815	6.0668

T=313.15 K

0.0000	-170284.8837	0.8594	0.0637	3.6978	0.0000	-178896.9490	0.9029	0.0648	3.7187
-0.0771	-209410.9805	1.1781	0.0760	3.9201	-0.0945	-220547.1074	1.2407	0.0770	3.9379
-0.1430	-249077.5447	1.5430	0.0874	4.1083	-0.1751	-262906.3476	1.6287	0.0884	4.1240
-0.1944	-288616.5739	1.9507	0.0984	4.2735	-0.2381	-305210.9693	2.0628	0.0994	4.2877
-0.2270	-325311.4235	2.3710	0.1084	4.4142	-0.2780	-344485.0280	2.5108	0.1094	4.4273
-0.2468	-407926.6262	3.4808	0.1314	4.7055	-0.3022	-432720.1667	3.6924	0.1323	4.7167
-0.2314	-484831.9858	4.7202	0.1531	4.9515	-0.2834	-514693.3541	5.0109	0.1540	4.9613
-0.2009	-558132.7394	6.0885	0.1740	5.1677	-0.2460	-592704.6321	6.4656	0.1749	5.1765
-0.1675	-622269.9982	7.4364	0.1925	5.3447	-0.2051	-660896.4061	7.8980	0.1934	5.3528
-0.1284	-700178.9073	9.2484	0.2148	5.5434	-0.1572	-743775.8743	9.8242	0.2156	5.5509
-0.1046	-743812.3862	10.3515	0.2273	5.6491	-0.1281	-790169.9457	10.9967	0.2282	5.6562
-0.0820	-783647.4653	11.4150	0.2388	5.7425	-0.1004	-832512.2900	12.1268	0.2396	5.7494
-0.0458	-848501.0593	13.2578	0.2574	5.8883	-0.0560	-901463.0830	14.0854	0.2583	5.8948
-0.0196	-895667.5272	14.6842	0.2710	5.9899	-0.0241	-951619.2411	15.6016	0.2718	5.9962
0.0000	-930831.3233	15.7949	0.2811	6.0635	0.0000	-989010.7055	16.7821	0.2819	6.0695

T=318.15 K

0.0000	-161805.4271	0.8215	0.0626	3.6750	0.0000	-169314.5044	0.8596	0.0637	3.6960
-0.0864	-199750.5098	1.1295	0.0750	3.9041	-0.1058	-209592.7116	1.1851	0.0761	3.9220
-0.1617	-238544.1825	1.4845	0.0867	4.0968	-0.1980	-250924.9450	1.5616	0.0877	4.1127
-0.2210	-277405.0909	1.8828	0.0978	4.2652	-0.2706	-292424.3676	1.9847	0.0988	4.2795
-0.2587	-313539.4257	2.2943	0.1080	4.4080	-0.3168	-331032.8021	2.4223	0.1090	4.4212
-0.2821	-394744.7597	3.3802	0.1311	4.7022	-0.3455	-417617.8569	3.5761	0.1320	4.7135

-0.2659	-470388.0325	4.5945	0.1529	4.9498	-0.3256	-498124.3414	4.8654	0.1538	4.9598
-0.2323	-542492.4455	5.9362	0.1739	5.1672	-0.2844	-574751.8323	6.2892	0.1749	5.1761
-0.1945	-605505.6083	7.2576	0.1925	5.3449	-0.2381	-641647.5164	7.6907	0.1934	5.3532
-0.1497	-682140.7266	9.0359	0.2149	5.5444	-0.1833	-723056.2924	9.5778	0.2158	5.5520
-0.1223	-725042.7620	10.1186	0.2275	5.6504	-0.1497	-768607.0219	10.7266	0.2283	5.6576
-0.0962	-764212.6984	11.1626	0.2390	5.7441	-0.1178	-810182.9556	11.8341	0.2398	5.7511
-0.0540	-827982.7786	12.9722	0.2577	5.8904	-0.0661	-877884.8679	13.7540	0.2585	5.8970
-0.0233	-874318.1901	14.3724	0.2713	5.9923	-0.0285	-927083.2029	15.2398	0.2721	5.9986
0.0000	-908837.1818	15.4624	0.2814	6.0659	0.0000	-963731.7598	16.3963	0.2823	6.0721

 $T=323.15$ K

0.0000	-153663.7313	0.8152	0.0613	3.6492	0.0000	-160160.0427	0.8287	0.0623	3.6702
-0.0989	-190614.3122	1.1215	0.0740	3.8865	-0.1212	-199280.9732	1.1457	0.0750	3.9044
-0.1838	-228540.6163	1.4749	0.0859	4.0843	-0.2251	-239595.1127	1.5137	0.0869	4.1002
-0.2500	-266639.9866	1.8715	0.0972	4.2560	-0.3061	-280196.0389	1.9285	0.0982	4.2704
-0.2921	-302121.1458	2.2815	0.1075	4.4010	-0.3576	-318034.0969	2.3581	0.1085	4.4143
-0.3192	-381921.1857	3.3638	0.1308	4.6984	-0.3909	-402976.1005	3.4922	0.1317	4.7097
-0.3021	-456312.4649	4.5744	0.1527	4.9478	-0.3699	-482028.9263	4.7612	0.1536	4.9578
-0.2650	-527216.6415	5.9120	0.1739	5.1664	-0.3245	-557269.7824	6.1633	0.1748	5.1754
-0.2228	-589152.7388	7.2295	0.1925	5.3449	-0.2728	-622925.0504	7.5438	0.1934	5.3532
-0.1719	-664508.1158	9.0028	0.2150	5.5452	-0.2105	-702858.4292	9.4037	0.2159	5.5528
-0.1408	-706708.3162	10.0826	0.2276	5.6515	-0.1724	-747600.9464	10.5365	0.2285	5.6588
-0.1110	-745226.1882	11.1238	0.2391	5.7456	-0.1360	-788426.6079	11.6286	0.2400	5.7526
-0.0625	-807915.7855	12.9284	0.2579	5.8922	-0.0766	-854885.1145	13.5217	0.2588	5.8989
-0.0270	-853456.2278	14.3249	0.2716	5.9944	-0.0331	-903168.6157	14.9870	0.2724	6.0008
0.0000	-887343.7008	15.4119	0.2817	6.0683	0.0000	-939090.9440	16.1272	0.2826	6.0745

Table 8 Infrared absorbance wave numbers (cm^{-1}) between 2800 to 3200 of [Bmim][NTf₂] in DMC at room temperature and atmospheric pressure $P = 101.3$ kPa.

Infrared absorbance wave numbers / cm^{-1}					
Mole fraction of [Bmim][NTf ₂]	Mole fraction of DMC	C ₂ -H stretching	C _{4,5} -H stretching	SO ₂ Sym Stretch	CF ₃ Sym Stretch
1.0000	0.0000	3120.7	3157.2	1131.5	1226.1
0.8990	0.1010	3120.7	3157.5	1131.7	1226.4
0.8055	0.1945	3120.7	3157.7	1132.0	1226.6
0.7006	0.2994	3120.7	3158.0	1132.3	1226.7
0.6001	0.3999	3119.5	3157.0	1132.5	1226.9
0.5024	0.4976	3120.2	3157.0	1133.0	1226.9
0.4158	0.5842	3120.2	3157.0	1133.8	1227.0
0.3114	0.6886	3119.9	3157.8	1134.1	1227.1
0.2525	0.7475	3118.3	3156.7	1135.1	1227.2
0.1110	0.8890	3118.1	3156.3	1137.0	1227.2
0.0000	1.0000	-	-	-	-

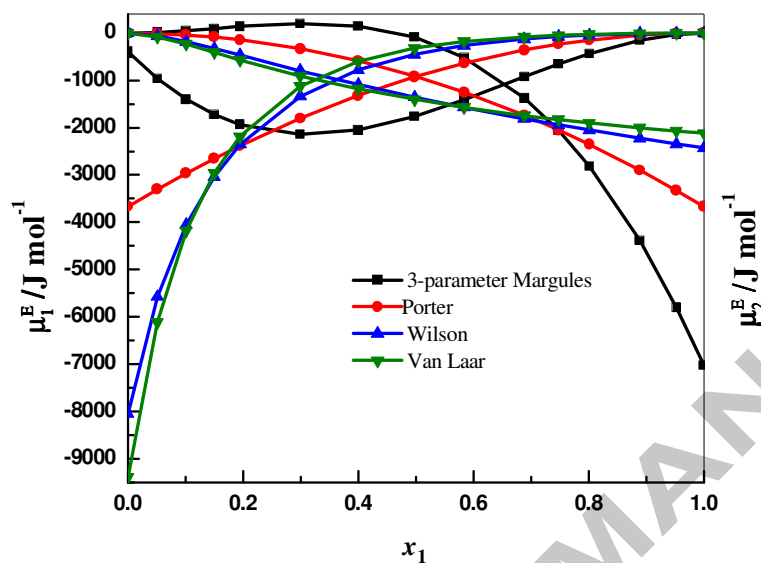
Table 9 Characteristic and reduced parameters for the pure components used in PFP theory at various temperatures.

T/K	\bar{v}	V_1^* / $10^{-6} \text{ m}^3 \cdot \text{mol}^{-1}$	P_1^* / $10^6 \text{ J} \cdot \text{mol}^{-1}$
[Bmim][NTf₂]			
303.15	1.1788	248.97	520.66
308.15	1.1813	249.28	520.50
313.15	1.1838	249.59	520.16
318.15	1.1862	249.91	519.73
323.15	1.1887	250.23	519.19
DMC			
303.15	1.3015	65.491	687.24
308.15	1.3082	65.569	685.34
313.15	1.3149	65.651	682.36
318.15	1.3217	65.737	677.89
323.15	1.3285	65.828	673.69

Table 10 PFP interaction parameter, χ_{12} , and calculated values of the three contributions from the PFP theory at equimolar composition for ([Bmim][NTf₂] + DMC) system at T=(303.15-323.15)K

T	χ_{12}	V_m^E/int	V_m^E/fv	V_m^E/ip
/K	/10 ⁶ J·m ⁻³	/ $10^{-6} \text{ m}^3 \cdot \text{mol}^{-1}$		
303.15	-63.1996	1.2105	-0.6834	0.9516
308.15	-63.1190	-1.2405	-0.7298	0.9758
313.15	-62.7714	-1.2664	-0.7780	0.9951
318.15	-61.9954	-1.2847	-0.8278	1.0058
323.15	-61.3045	-1.3047	-0.8800	1.0181

Graphical abstract



Highlights

- The studied binary system is {[Bmim][NTf₂]+DMC}
- Density, speed of sound and refractive index are measured at various temperatures
- Derived excess/deviation parameters indicated the existence of strong interactions
- Acoustic non-linearity parameter , cohesive energy etc., are evaluated
- IR spectra and PFP theory also support the existence of strong interactions